Steel and Composite Structures, *Vol. 32, No. 2 (2019) 157-171*
DOI: https://doi.org/10.12989/scs.2019.32.2.157

Dynamic instability region analysis of sandwich piezoelectric nano-beam with FG-CNTRCs face-sheets based on various high-order shear deformation and nonlocal strain gradient theory

Mohammad Arefi *, Mahmoud Pourjamshidian [a] and Ali Ghorbanpour Arani [b]

Department of Solid Mechanics, Faculty of Mechanical Engineering, University of Kashan, Postal Code 87317-53153, Kashan, Iran

(*Received January 30, 2018, Revised November 22, 2018, Accepted November 28, 2018*)

Abstract. In this research, the dynamic instability region (DIR) of the sandwich nano-beams are investigated based on nonlocal strain gradient elasticity theory (NSGET) and various higher order shear deformation beam theories (HSDBTs). The sandwich piezoelectric nano-beam is including a homogenous core and face-sheets reinforced with functionally graded (FG) carbon nanotubes (CNTs). In present study, three patterns of CNTs are employed in order to reinforce the top and bottom face-sheets of the beam. In addition, different higher-order shear deformation beam theories such as trigonometric shear deformation beam theory (TSDBT), exponential shear deformation beam theory (ESDBT), hyperbolic shear deformation beam theory (HSDBT), and Aydogdu shear deformation beam theory (ASDBT) are considered to extract the governing equations for different boundary conditions. The beam is subjected to thermal and electrical loads while is resting on Visco-Pasternak foundation. Hamilton principle is used to derive the governing equations of motion based on various shear deformation theories. In order to analysis of the dynamic instability behaviors, the linear governing equations of motion are solved using differential quadrature method (DQM). After verification with validated reference, comprehensive numerical results are presented to investigate the influence of important parameters such as various shear deformation theories, nonlocal parameter, strain gradient parameter, the volume fraction of the CNTs, various distributions of the CNTs, different boundary conditions, dimensionless geometric parameters, Visco-Pasternak foundation parameters, applied voltage and temperature change on the dynamic instability characteristics of sandwich piezoelectric nano-beam.

Keywords: shear deformation theory; reinforcement CNTs composite; sandwich nano-beam; nonlocal strain gradient theory; dynamic instability region

1. Introduction

Since CNTs have very surprising properties, they are used to make composite materials for the development of properties of other materials. Therefore, composites made of CNTs have recently become widely used in a variety of industries, such as the aerospace industry, the construction industry and the mechanical engineering industry. The structures made of carbon nanotube reinforcement composite (CNTRC) have a very good and upgraded mechanical properties. Reinforcement of structures with carbon nanotubes leads to structures with high strength, high toughness, high ultimate strength and low density that encourage designer to reach best composition for special applications (Ke *et al*. 2010). Therefore, many researchers have recently investigated this topic in a variety of areas. As a result, progressive investigations with CNTs subjects have been ongoing in recent years. So that CNTs have found many applications in different fields such as mechanical and civil engineering (Rafiee *et al*. 2013). A comprehensive literature review on the CNTRC structures can be presented to enrich our work.

On the other hand, beams are one of the most important structural members in complex mechanical analysis (Arefi *et al*. 2017). There are different applications for beam in various engineering structures in macro, micro or nano scales. Therefore, for designing a structure, having an understanding of the behavior of the beam for the designer is inevitable. Due to the large application of these members in the construction of complex structures, many researchers have researched this topic (Reddy and El-Borgi 2014). In this regard, various theories were presented by investigators in order to different analyses of the beam structures in mentioned scales. Reddy were used different beams theories such as the Euler–Bernoulli, the first order shear deformation beam theory (FSDBT), Reddy or parabolic shear deformation beam theory (PSDBT) and Levinson beam theories based on the nonlocal differential constitutive relations of Eringen in his investigations (Reddy 2007). He accomplished the parametric investigation in order to study the effects of nonlocal parameter on buckling loads, natural frequencies and bending behaviors of the nano-beams.

In addition, the influences of the non-classical stiffness strengthening size effects on free vibration of a nonlocal Timoshenko beam (Yang and Lim 2012), nonlinear free

*Corresponding author, Ph.D., Assistant Professor,
E-mail: arefi63@gmail.com; arefi@kashanu.ac.ir
[a] Ph.D. Student
[b] Ph.D., Professor

ISSN: 1229-9367 (Print), 1598-6233 (Online)

vibration analysis of rotating composite Timoshenko beams (Arvin and Bakhtiari-Nejad 2013) and forced vibration analysis of Timoshenko nano-beams based on surface stress elasticity theory (Ansari *et al*. 2014c) were studied by various researchers in detail. In order to investigate the dynamic and static behaviors of the thick beams, other higher-order shear deformation beam theories (HOSBTs) has been developed so that aforementioned theories to take into account the influence of transverse shear deformation to best prediction of behavior of thick beams (Li *et al*. 2014, Zidi *et al*. 2014, Yahia *et al*. 2015, Bousahla *et al*. 2016, El-Haina *et al*. 2017). There are some other theories in relation to beams such as trigonometric shear deformation beam theory (TSDBT), exponential shear deformation beam theory (ESDBT), hyperbolic shear deformation beam theory (HSDBT), and Aydogdu shear deformation beam theory (ASDBT) (Simsek and Reddy 2013a, b, Boukhari *et al*. 2016).

The DIR and vibration behavior analysis of the macro and nano-beam with considering HOSDBTs and stretching effect is very practical and interest topic that has been studied by many researchers (Bousahla *et al*. 2014, Bennoun *et al*. 2016). Since piezoelectric beams have found many applications in the electronic industry, many researchers have investigated the dynamical behavior of these important structural members. Kolahchi et al. a model for dynamic instability of embedded single-walled carbon nanotubes (SWCNTs) was presented (Kolahchi and Moniri Bidgoli 2016). They were modeled SWCNTs by the sinusoidal shear deformation beam theory (SSDBT) and also the modified couple stress theory (MCST) was considered in order to capture the size effects. The results presented in their investigation depicted that increasing the nonlocal parameter shifts the DIR to right. The thermo-piezoelectric buckling, nonlinear free vibration and dynamic stability for the piezoelectric functionally graded beams, subjected to one-dimensional steady heat conduction in the thickness direction, were studied by Fu et al. (Fu *et al*. 2012). The effects of the thermal load, electric load, and thermal properties of the constituent materials on the thermo-piezoelectric buckling, nonlinear free vibration, and dynamic stability of the piezoelectric functionally graded beam were discussed, and some meaningful conclusions have been drawn. The nonlinear dynamic stability analysis of embedded temperature-dependent viscoelastic plates reinforced by single-walled carbon nanotubes (SWCNTs) was investigated by Kolahchi *et al*. (2016). The static, dynamic, and buckling behavior of partial interaction composite members was investigated by taking into account for the influences of rotary inertia and shear deformations (Xua and Wu 2007). Chen *et al*. (2002) the slender laminated composite beam with piezoelectric layers subjected to axial periodic compressive loads was considered and dynamic stability behaviors of aforementioned structure were investigated. They was evaluated the influence of the feedback control gain on the response of the beam. According to obtained results, they indicated that the small scale parameter, elastic medium, temperature change and electric potential have significantly effect on the dimensionless natural frequency and critical fluid velocity. Furthermore, the effect of fluid viscosity on the vibration of DWBNNTs may be ignored. In another investigation Ghorbanpour Arani et al. studied the control and analyze the nonlinear dynamic stability of single layered graphene sheets (SLGSs) integrated with Zinc oxide (ZnO) actuators and sensors (Ghorbanpour Arani *et al*. 2015b). They concluded that the magnetic field and external voltage are effective controlling parameters for DIR of system. Nonlinear analysis of functionally graded plates was studied by Arefi and Allam (2015).

Use of composite materials causes the increase in quality of the mechanical and physical behaviors and response of structures. Carbon nanotube reinforcement composites (CNTRCs) are one of the best known composite materials that have recently been featured. Aforementioned composite materials can be used to reinforce the polymer composites (Esawi and Farag 2007). improving and developing the materials propertied with CNTs makes that the CNTRCs achieve a wide applications in micro and nano systems (Ashrafi and Hubert 2006). These materials have been widely used in the design and construction of nano-electro-mechanical systems (NEMS)/micro-electro-mechanical systems (MEMS) (Ghorbanpour Arani et al. 2012a, c). That's why; many researchers focused on the problems that concern with FG-CNTRC and they studied various problems related to these topics. For example thermal stresses analysis; linear and nonlinear vibration and dynamic responses of various structures in thermal environments were studied by some researchers (Ghorbanpour Arani *et al*. 2012b, 2015a). The influences of the various pattern of the of SWCNTs as: UD, FG-V, FG-X and FG-O on dimensionless natural frequency of visco-elastic double-bonded polymeric nano-composite plate was studied by Mohammadimehr *et al*. (2015). They have concluded that application of micro/nano-composites in micro/nano electromechanical systems leads to important and novel responses to raised problem in this context. In other work, Wu *et al*. (2017) investigated the imperfection sensitivity of thermal post-buckling behavior of functionally graded carbon nanotube-reinforced composite (FG-CNTRC) beams subjected to in-plane temperature variation. Rafiee et al. carried out an investigation on nonlinear stability and resonance response of the imperfect plate made of piezoelectric FG-CNTRC subjected to various combined electrical and thermal loads (Rafiee *et al*. 2014). The free vibration behavior of the pre-twisted functionally graded carbon nanotube reinforced composite (FG-CNTRC) beams in thermal environment was studied by Ghorbani Shenas *et al*. (2017).

The effects of the small scales in micro and nano structures are the main parameters that they should be considered to extract the governing equations of the engineering structures in order to have a precise mechanical behaviors analysis (Amine *et al*. 2015, Hichem *et al*. 2017). Therefore in whole of the investigations related to small scale structures topic in order to incorporate the small scales in equations of motions, various theories such as the strain gradient theory and Eringen's differential nonlocal model were used (Khetir *et al*. 2017). In the other hand, Classical continuum models (Zhang and Paulino 2007), nonlocal

continuum theory (Ebrahimy and Hosseini 2016), strain gradient theory, and modified couple stress models (Ansari *et al*. 2014b) have been used by researchers for analysis of nano/micro systems. Generally, based on the nonlocal continuum theory the stress at a specified point of the body depend on the strains at other near points (Eringen 1983). Based on the nonlocal strain gradient theory, Liew *et al*. (2008) analyzed the wave propagation in a SWCNT by molecular dynamics simulations. Combination of above mentioned aspects of beams leads to an interesting problem in scope of mechanical engineering and nano-mechanical-systems.

Regard to literature review mentioned above and author's knowledge, we can conclude that there is no published work about the DIR of the sandwich nano-beams based on NSGET and various HSDBTs. In this study, the sandwich piezoelectric nano-beam is including a homogenous core and face-sheets reinforced with FG-CNTs. Also, three patterns of CNTs are employed in order to reinforce the top and bottom face-sheets of the beam and different HOSDBTs such as TSDBT, ESDBT, HSDBT, and ASDBT are considered to extract the governing equations. The beam is subjected to thermal and electrical loads while is resting on Visco-Pasternak foundation. After verification of the obtained results with validated reference, comprehensive numerical results are presented to investigate the influence of important parameters such as various shear deformation theories, nonlocal parameter, strain gradient parameter, the volume fraction of the CNTs, various distributions of the CNTs, different boundary conditions, dimensionless geometric parameters, Visco-Pasternak foundation parameters, applied voltage and temperature change on the dynamic instability characteristics of sandwich piezoelectric nano-beam.

2. Material properties of Sandwich FG-CNTRC nano-beams

The schematic of the structure studied in this research is presented in Fig. 1. According to this figure, the sandwich nano-beam is made of two FG-CNTRC face-sheets and a homogenous piezoelectric core. In this section, the material properties of core and two face-sheets are expressed and calculated in detail. Also, this can be seen in Fig. 2, the CNTs are aligned along thickness direction of the face-sheets with three patterns named FG(AV), FG(VA) and UD. Also it is assumed that the material of the core and face-sheets matrix have the piezoelectric properties.

In order to calculate effective material properties of the CNTRCs, the total volume can be defined as (Tornabene *et al*. 2017)

$$W = W_{CN} + W_m \tag{1}$$

In which, W_{CN} and W_m are the volume of the reinforcing phase and matrix, respectively. Also, the mass fraction of nanoparticles w_{CN} and the mass fraction of the polymer matrix w_m are calculated as the following form (Tornabene *et al*. 2016)

$$\begin{aligned} w_{CN} &= \frac{M_{CN}}{M_{CN} + M_m}, \\ w_m &= \frac{M_m}{M_{CN} + M_m}, \end{aligned} \tag{2}$$

In which, M_{CN} and M_m characterize the CNTs and the matrix masses, respectively. At this point, the volume fraction of the CNTs and matrix is defined as

$$\begin{aligned} V_{CN} &= \frac{W_{CN}}{W}, \\ V_m &= \frac{W_m}{W}, \end{aligned} \tag{3}$$

To calculate the effective properties of CNTRC, the Mori–Tanaka scheme or the rule of mixtures can be used (Natarajan *et al*. 2014). In this investigation to compute the effective material properties of face-sheets, the rule of mixtures with correction factors is employed. The properties of the CNTRC (Young's modulus (E^{rc}) and density (ρ^{rc}) of the reinforced composite) are expressed as (Rafiee *et al*. 2014)

$$\begin{aligned} E^{rc} &= \eta_1 V_{cn} E_{11}^{CN} + V_m E^m \\ G^{rc} &= \eta_1 V_{cn} G^{CN} + V_m G^m \\ \rho^{rc} &= V_{cn} \rho^{CN} + V_m \rho^m \end{aligned} \tag{4}$$

In which, η_1, E_{11}^{CN}, G^{CN}, α_{11}^{CN} and ρ_{11}^{CN} are the CNT efficiency parameter, the Young's modulus, the shear modulus, the expansion coefficient and density of the CNTs, respectively and E^m, G^m, α^m and ρ^m are the corresponding properties for the matrix. It is noted that superscript rc and m denotes the reinforcement composite and matrix, respectively. In addition, V_{CN} and

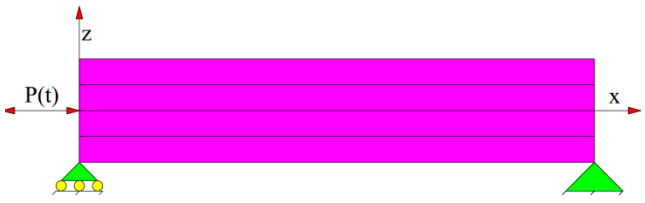

Fig. 1 Sandwich piezoelectric nano-beam with FG-CNTRC face-sheets

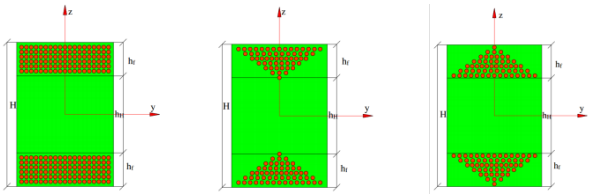

UU Pattern VA Pattern AV Pattern

Fig. 2 Sandwich piezoelectric nano-beam with FG-CNTRC face-sheets

V_m are related by relation $V_{CN} + V_m = 1$ (Shen and Zhang 2012, Tornabene *et al*. 2017). According to investigations accomplished by Tornabene *et al*. (2016) if the through-the-thickness distribution is represented by V_{CN}^d, the gradual variation of the nanoparticles along the normal direction $\bar{z}$ for every layer is given by

$$V_{CN} = V_{CN}^* V_{CN}^d \tag{5}$$

Where, V_{CN}^* can be calculated as the following form

$$V_{CN}^* = \frac{w_{CN}}{w_{CN} + \left(\frac{\rho^{CN}}{\rho^m}\right) - \left(\frac{\rho^{CN}}{\rho^m}\right) w_{CN}} \tag{6}$$

It is worthy noted that since the present approach is general, there is no limitation on the choice of V_{CN}^d (Fantuzzia *et al*. 2017). The three distributions of the CNTs along the face-sheets are introduced as

$$\begin{aligned}
&V_{CN}^t = 2\frac{(t_2 - \bar{z})}{(t_2 - t_3)} V_{CN}^* \\
&V_{CN}^b = 2\frac{(t_1 + \bar{z})}{(t_1 - t_0)} V_{CN}^*, \quad \Rightarrow \quad \textit{for FG(VA) pattern} \\
&V_{CN}^t = V_{CN}^* \\
&V_{CN}^b = V_{CN}^*, \quad \Rightarrow \quad \textit{for UD pattern} \\
&V_{CN}^t = 2\frac{(t_3 - \bar{z})}{(t_3 - t_2)} V_{CN}^* \\
&V_{CN}^b = 2\frac{(t_0 + \bar{z})}{(t_0 - t_1)} V_{CN}^*, \quad \Rightarrow \quad \textit{for FG(AV) pattern}
\end{aligned} \tag{7}$$

In which V_{CN}^t and V_{CN}^b represent the volume fractions of the CNTs in top and bottom face-sheets, respectively.

3. Formulation

The displacement field based on HOSDBTs is expressed as

$$\begin{aligned}
&\bar{u}(\bar{x}, \bar{z}, \bar{t}) = u_0(\bar{x}, \bar{t}) - \bar{z}\frac{\partial w_0(\bar{x}, \bar{t})}{\partial \bar{x}} + \varphi(\bar{z})\gamma(\bar{x}, \bar{t}) \\
&\bar{w}(\bar{x}, \bar{z}, \bar{t}) = w_0(\bar{x}, \bar{t})
\end{aligned} \tag{8}$$

In which, u and w are the axial and transverse displacements, u_0 and w_0 are displacement components of the mid-surface along the axial and transverse directions. In addition $\varphi(z)$ is a function of z that presents the transverse shear and stress distribution along the thickness of the nano-beam (Simsek and Reddy 2013a, b, Arefi and Zenkour 2017a-h). According to accomplished study, $\varphi(z)$ is defined for FSDBT as z, PSDBT as $z\left(1 - \frac{4z^2}{3H^2}\right)$, TSDBT as $\frac{H}{\pi}\sin\left(\frac{\pi z}{H}\right)$, HSDBT as $H\sin\left(\frac{z}{H}\right) - z\cosh\left(\frac{1}{2}\right)$, ESDBT as $z\exp\left(-2\left(\frac{z}{H}\right)^2\right)$ and also for new HOSDBT as the following form (Li *et al*. 2014, Arefi and Zenkour 2017a-i)

$\varphi(z)$	New theory
$z\alpha^{\frac{-2\left(\frac{z}{H}\right)^2}{\ln\alpha}}$ *in which* $\alpha = 3$	ASDBT

(9)

Also in Eq. (8) $\gamma(\bar{x}, \bar{t})$ is the transverse shear strain of any point on the neutral axis (Simsek and Reddy 2013a, b) and is specified as

$$\gamma(\bar{x}, \bar{t}) = \phi(\bar{x}, \bar{t}) + \frac{\partial w_0(\bar{x}, \bar{t})}{\partial \bar{x}} \tag{10}$$

In Eq. (10), $\phi(\bar{x}, \bar{t})$ is the total bending rotation of the cross sections at any point on the neutral axis. The strain-displacement relation with considering the thermal strain is expressed as

$$\begin{aligned}
&\varepsilon_{\bar{x}\bar{x}} = \frac{\partial u_0}{\partial \bar{x}} - \bar{z}\frac{\partial^2 w_0}{\partial \bar{x}^2} + \varphi\left(\frac{\partial^2 w_0}{\partial \bar{x}^2} - \frac{\partial \phi}{\partial \bar{z}}\right) - \alpha(\bar{z})\Delta T \\
&\varepsilon_{\bar{x}\bar{z}} = \frac{\partial \varphi}{\partial \bar{z}}\left(\frac{\partial w_0}{\partial \bar{x}} - \phi\right)
\end{aligned} \tag{11}$$

In which, ΔT is the increment of temperature from the initial temperature (T_0) that is equal to $\Delta T = T - T_0$. In the present study, it is assumed that the electric potential as a sum of a cosine and linear variation. Then the electric potential can be written as (Arefi *et al*. 2018, Arefi and Zenkour 2017a-i, 2018)

$$\tilde{\Phi}(\bar{x}, \bar{z}, \bar{t}) = \cos(\beta\bar{z})\bar{\Phi}(\bar{x}, \bar{t}) + \frac{2\bar{z}V_0}{h} \tag{12}$$

In Eq. (12), $\beta = \frac{\pi}{h}$ and also $\bar{\Phi}(\bar{x}, \bar{t})$ is electric potential distribution along the longitudinal direction (Ke *et al*. 2010); V_0 is the external electric voltage (Liew *et al*. 2003). It is noted that $\bar{\Phi}(\bar{x}, \bar{t})$ must satisfy the homogeneous electric boundary conditions. Regard to Eq. (12), the electric fields can be defined as (Arefi 2016, Arefi et al. 2018, Arefi and Zenkour 2017a-i, 2018)

$$\begin{aligned}
&E_{\bar{x}} = -\frac{\partial \tilde{\Phi}}{\partial \bar{x}} = -\cos(\beta\bar{z})\frac{\partial \bar{\Phi}}{\partial \bar{x}} \\
&E_{\bar{z}} = -\frac{\partial \tilde{\Phi}}{\partial \bar{z}} = \beta\sin(\beta\bar{z})\bar{\Phi}(\bar{x}, \bar{t}) - E_0, \qquad E_0 = \frac{2V_0}{h}
\end{aligned} \tag{13}$$

The strain-stress relation for reinforcement composite face-sheets defined as (Li *et al*. 2015)

$$\begin{aligned}
&\sigma_{\bar{x}\bar{x}}^f = E^f(\bar{z})\left(\frac{\partial u_0}{\partial \bar{x}} - \bar{z}\frac{\partial^2 w_0}{\partial \bar{x}^2} + \varphi\left(\frac{\partial^2 w_0}{\partial \bar{x}^2} - \frac{\partial \phi}{\partial \bar{z}}\right) - \right. \\
&\left. \alpha(\bar{z})\Delta T\right) \\
&\sigma_{\bar{x}\bar{z}}^f = G^f(\bar{z})\frac{\partial \varphi}{\partial \bar{z}}\left(\frac{\partial w_0}{\partial \bar{x}} - \phi\right)
\end{aligned} \tag{14}$$

In general, the properties associated with the core and face-sheets represent with *p* and *f* superscripts, respectively. Taking into account the voltage applied on piezoelectric core layer, the constitutive relations relation of the core is specified as

$$\begin{aligned}\sigma_{\bar{x}\bar{x}}^{p} &= E^{p}\left(\begin{array}{l}\dfrac{\partial u_0}{\partial \bar{x}} - \bar{z}\dfrac{\partial^2 w_0}{\partial \bar{x}^2} + \varphi\left(\dfrac{\partial^2 w_0}{\partial \bar{x}^2} - \dfrac{\partial \phi}{\partial \bar{z}}\right) - \\ \alpha(\bar{z})\Delta T\end{array}\right) - \\ & e_{31}E_{\bar{z}} \\ \sigma_{\bar{x}\bar{z}}^{p} &= G^{p}\frac{\partial \varphi}{\partial \bar{z}}\left(\frac{\partial w_0}{\partial \bar{x}} - \phi\right) - e_{15}E_{\bar{x}} \\ D_{\bar{x}} &= e_{15}\varepsilon_{\bar{x}\bar{z}} - k_{11}E_{\bar{x}} \\ D_{\bar{z}} &= e_{31}\varepsilon_{\bar{x}\bar{x}} - k_{33}E_{\bar{z}}\end{aligned} \tag{15}$$

In which, $D_{\bar{x}}$ and $D_{\bar{z}}$ represent the electric displacement. In addition, e_{31}, e_{15} are the piezoelectric constants and also k_{11}, k_{33} are the dielectric constants (Liew *et al*. 2003, Rafiee *et al*. 2013). The Hamilton's principle is used to drive governing equation of motion as (Komijani *et al*. 2014)

$$0 = \int_0^T \left(\delta T - \delta U_s - \delta U_f + \delta W\right) d\bar{t} \tag{16}$$

Where δU_s, δU_f, δT and δW are the variations of strain energy, foundation reaction, kinetic energy and external works, respectively. Variation of strain energy δU_s is calculated as

$$\delta U_s = \int_0^L \int_A \left(\sigma_{\bar{x}\bar{x}}\delta\varepsilon_{\bar{x}\bar{x}} + \sigma_{\bar{x}\bar{z}}\delta\varepsilon_{\bar{x}\bar{z}} - D_{\bar{x}}E_{\bar{x}} - D_{\bar{z}}E_{\bar{z}}\right) dA d\bar{x} \tag{17}$$

Variation of kinetic energy is represented as

$$\delta T = \int_0^L \int_A \rho(\bar{z})\left(\frac{\partial \bar{u}}{\partial \bar{t}}\frac{\partial \bar{u}}{\partial \bar{t}} + \frac{\partial \bar{w}}{\partial \bar{t}}\frac{\partial \bar{w}}{\partial \bar{t}}\right) dA d\bar{x} \tag{18}$$

Variations of work done by the external forces and the linear elastic foundation are written as (Ghorbanpour Arani *et al*. 2012a, Kanani *et al*. 2014, Komijani *et al*. 2014)

$$\begin{aligned}\delta W &= \int_0^L \left(F\delta u_0 + Q\delta w_0 + \bar{N}_0\frac{\partial w_0}{\partial \bar{x}}\frac{\partial \delta w_0}{\partial \bar{x}}\right) d\bar{x} \\ \delta U_f &= \int_0^L \int_0^b \left(\bar{K}_w w_0 \delta w_0 + \bar{K}_s\frac{\partial w_0}{\partial \bar{x}}\delta\left(\frac{\partial w_0}{\partial \bar{x}}\right)\right) d\bar{y} d\bar{x} - \\ & b\int_0^L \bar{C}_d\frac{\partial w}{\partial \bar{t}} dx\end{aligned} \tag{19}$$

Where F and Q are the axial and transverse forces per unit length respectively and $\bar{N}_0$ is the axial compressive or pretension force. Also, $\bar{K}_w$, $\bar{K}_s$ and $\bar{C}_d$ are linear spring, shear and damping coefficient of foundation, respectively. Substituting Eqs. (8)-(11) into Eqs. (17)-(19) and consequently into Eq. (16), yields the governing equations of motions as

$$\begin{aligned}&\delta u_0 : \frac{\partial N_{\bar{x}}}{\partial \bar{x}} + F = \bar{I}_A\frac{\partial^2 u_0}{\partial \bar{t}^2} - \bar{I}_{B1}\frac{\partial^3 w_0}{\partial \bar{t}^2 \partial \bar{x}} + \bar{I}_{B2}\frac{\partial^3 w_0}{\partial \bar{t}^2 \partial \bar{x}} - \\ &\qquad \bar{I}_{B2}\frac{\partial^2 \phi}{\partial \bar{t}^2} \\ &\delta w_0 : \frac{\partial^2 M_{\bar{x}}}{\partial \bar{x}^2} - \frac{\partial^2 M_{\bar{x}}^{h}}{\partial \bar{x}^2} + \frac{\partial}{\partial \bar{x}}\left(N_{\bar{x}}\frac{\partial w_0}{\partial \bar{x}}\right) + \frac{\partial Q_{\bar{x}\bar{z}}}{\partial \bar{x}} - \\ &\bar{K}_w w_0 + \bar{K}_s\frac{\partial^2 w_0}{\partial \bar{x}^2} - \bar{C}_d\frac{\partial w_0}{\partial \bar{t}} + Q = \bar{I}_{B1}\frac{\partial^3 u_0}{\partial \bar{x}\partial \bar{t}^2} - \\ &\bar{I}_{B2}\frac{\partial^3 u_0}{\partial \bar{x}\partial \bar{t}^2} + \bar{I}_A\frac{\partial^2 w_0}{\partial \bar{t}^2} - \bar{I}_{D1}\frac{\partial^4 w_0}{\partial \bar{t}^2 \partial \bar{x}^2} + \bar{I}_{D2}\frac{\partial^4 w_0}{\partial \bar{t}^2 \partial \bar{x}^2} + \\ &\bar{I}_{D2}\frac{\partial^4 w_0}{\partial \bar{t}^2 \partial \bar{x}^2} - \bar{I}_{D3}\frac{\partial^4 w_0}{\partial \bar{t}^2 \partial \bar{x}^2} - \bar{I}_{D2}\frac{\partial^3 \phi}{\partial \bar{x}\partial \bar{t}^2} + \bar{I}_{D3}\frac{\partial^3 \phi}{\partial \bar{x}\partial \bar{t}^2} \\ &\delta\phi : Q_{\bar{x}\bar{z}} - \frac{\partial M_{\bar{x}}}{\partial \bar{x}} = \bar{I}_{B2}\frac{\partial^2 u_0}{\partial \bar{t}^2} + \bar{I}_{D2}\frac{\partial^3 w_0}{\partial \bar{t}^2 \partial \bar{x}} - \bar{I}_{D3}\frac{\partial^3 w_0}{\partial \bar{t}^2 \partial \bar{x}} \\ &\qquad + \bar{I}_{D3}\frac{\partial^2 \phi}{\partial \bar{t}^2} \\ &\delta\xi : \int_A \left(\cos(\beta\bar{z})\frac{\partial \bar{D}_{\bar{x}}}{\partial \bar{x}} - \beta\sin(\beta\bar{z})\bar{D}_{\bar{z}}\right) dA = 0\end{aligned} \tag{20}$$

Where, $N_{\bar{x}}$, $Q_{\bar{x}\bar{z}}$, $M_{\bar{x}}$ and $M_{\bar{x}}^{h}$ the resultants of forces and the moments. They are expressed as

$$\begin{aligned}N_{\bar{x}} &= \int_{-h/2}^{h/2}\sigma_{\bar{x}\bar{x}}(\bar{z})d\bar{z} = \\ &\left(\int_{t_0}^{t_1}\sigma_{\bar{x}\bar{x}}^{f}d\bar{z} + \int_{t_1}^{t_2}\sigma_{\bar{x}\bar{x}}^{p}d\bar{z} + \int_{t_2}^{t_3}\sigma_{\bar{x}\bar{x}}^{f}d\bar{z}\right) \\ Q_{\bar{x}\bar{z}} &= \int_{-h/2}^{h/2}\frac{\partial \varphi(\bar{z})}{\partial \bar{x}}\sigma_{\bar{x}\bar{z}}(\bar{z})d\bar{z} = \\ &\left(\int_{t_0}^{t_1}\frac{\partial \varphi(\bar{z})}{\partial \bar{x}}\sigma_{\bar{x}\bar{x}}^{f}d\bar{z} + \int_{t_1}^{t_2}\frac{\partial \varphi(\bar{z})}{\partial \bar{x}}\sigma_{\bar{x}\bar{x}}^{p}d\bar{z} + \int_{t_2}^{t_3}\frac{\partial \varphi(\bar{z})}{\partial \bar{x}}\sigma_{\bar{x}\bar{x}}^{f}d\bar{z}\right) \\ M_{\bar{x}} &= \int_{-h/2}^{h/2}\bar{z}\sigma_{\bar{x}\bar{x}}(\bar{z})d\bar{z} = \\ &\left(\int_{t_0}^{t_1}\bar{z}\sigma_{\bar{x}\bar{x}}^{f}d\bar{z} + \int_{t_1}^{t_2}\bar{z}\sigma_{\bar{x}\bar{x}}^{p}d\bar{z} + \int_{t_2}^{t_3}\bar{z}\sigma_{\bar{x}\bar{x}}^{f}d\bar{z}\right) \\ M_{\bar{x}} &= \int_{-h/2}^{h/2}\varphi(\bar{z})\sigma_{\bar{x}\bar{x}}(\bar{z})d\bar{z} = \\ &\left(\int_{t_0}^{t_1}\varphi(\bar{z})\sigma_{\bar{x}\bar{x}}^{f}d\bar{z} + \int_{t_1}^{t_2}\varphi(\bar{z})\sigma_{\bar{x}\bar{x}}^{p}d\bar{z} + \int_{t_2}^{t_3}\varphi(\bar{z})\sigma_{\bar{x}\bar{x}}^{f}d\bar{z}\right)\end{aligned} \tag{21}$$

The integration constants presented in Eq. (20) can be presented as

$$\begin{aligned}\bar{I}_A &= \int_{-h/2}^{h/2}\rho(\bar{z})d\bar{z} \\ \left\{\begin{array}{l}\bar{I}_{B1} \\ \bar{I}_{B2}\end{array}\right\} &= \int_{-h/2}^{h/2}\left\{\begin{array}{l}\bar{z} \\ \varphi(\bar{z})\end{array}\right\}\rho(\bar{z})d\bar{z} \\ \left\{\begin{array}{l}\bar{I}_{D1} \\ \bar{I}_{D2} \\ \bar{I}_{D3}\end{array}\right\} &= \int_{-h/2}^{h/2}\left\{\begin{array}{l}\bar{z}^2 \\ \bar{z}\varphi(\bar{z}) \\ \varphi(\bar{z})^2\end{array}\right\}\rho(\bar{z})d\bar{z}\end{aligned} \tag{22}$$

In according to nonlocal strain gradient theory (Li and Hu 2016), the constitutive relations are expressed as

$$\begin{aligned}
&\left(1-\left(\bar{e}_0\bar{a}\right)^2\nabla^2\right)\sigma_{\bar{x}\bar{x}}=E\left(z\right)\left(1-\bar{l}_m^{\,2}\nabla^2\right)\varepsilon_{\bar{x}\bar{x}}-\\
&\quad E\left(\bar{z}\right)\alpha\left(\bar{z}\right)\Delta T-e_{31}E_{\bar{z}}\\
&\left(1-\left(\bar{e}_0\bar{a}\right)^2\nabla^2\right)\sigma_{\bar{x}\bar{z}}=G\left(z\right)\left(1-\bar{l}_m^{\,2}\nabla^2\right)\varepsilon_{\bar{x}\bar{z}}-e_{15}E_{\bar{x}}\\
&\left(1-\left(\bar{e}_0\bar{a}\right)^2\nabla^2\right)D_{\bar{x}}=e_{15}\left(1-\bar{l}_m^{\,2}\nabla^2\right)\varepsilon_{\bar{x}\bar{z}}-k_{11}E_{\bar{x}}\\
&\left(1-\left(\bar{e}_0\bar{a}\right)^2\nabla^2\right)D_{\bar{z}}=e_{31}\left(1-\bar{l}_m^{\,2}\nabla^2\right)\varepsilon_{\bar{x}\bar{x}}-k_{33}E_{\bar{z}}
\end{aligned}\tag{23}$$

In Eq. (23), $\nabla^2=\partial^2/\partial\bar{x}^2$ is the Laplacian operator, $\bar{e}_0\bar{a}$ is the nonlocal parameter and $\bar{l}_m$ is the strain gradient length scale parameter. The nonlocal strain gradient constitutive relations in Eq. (23) can be written in an explicit form as follows

$$\begin{aligned}
&\sigma_{\bar{x}\bar{x}}-\left(\bar{e}_0\bar{a}\right)^2\frac{\partial^2\sigma_{\bar{x}\bar{x}}}{\partial\bar{x}^2}=\left(1-\bar{l}_m^{\,2}\nabla^2\right)E\left(\bar{z}\right)\times\\
&\quad\left[\frac{\partial u_0}{\partial\bar{x}}-\bar{z}\frac{\partial^2 w_0}{\partial\bar{x}^2}+\varphi\left(\frac{\partial^2 w_0}{\partial\bar{x}^2}-\frac{\partial\phi}{\partial\bar{z}}\right)\right]-\\
&\quad E\left(\bar{z}\right)\alpha\left(\bar{z}\right)\Delta T-e_{31}\left(\beta\sin\left(\beta\bar{z}\right)\bar{\Phi}\left(\bar{x},\bar{t}\right)-E_0\right)\\
&\sigma_{\bar{x}\bar{z}}-\left(\bar{e}_0\bar{a}\right)^2\frac{\partial^2\sigma_{\bar{x}\bar{z}}}{\partial\bar{x}^2}=\left(1-\bar{l}_m^{\,2}\nabla^2\right)G\left(\bar{z}\right)\times\\
&\quad\left[\frac{\partial\varphi}{\partial\bar{z}}\left(\frac{\partial w_0}{\partial\bar{x}}-\phi\right)\right]+e_{15}\left(\cos\left(\beta\bar{z}\right)\frac{\partial\bar{\Phi}}{\partial\bar{x}}\right)\\
&\left(1-\left(\bar{e}_0\bar{a}\right)^2\nabla^2\right)D_{\bar{x}}=e_{15}\left(1-\bar{l}_m^{\,2}\nabla^2\right)\times\\
&\quad\left[\frac{\partial\varphi}{\partial\bar{z}}\left(\frac{\partial w_0}{\partial\bar{x}}-\phi\right)\right]+k_{11}\left(\cos\left(\beta\bar{z}\right)\frac{\partial\bar{\Phi}}{\partial\bar{x}}\right)\\
&\left(1-\left(\bar{e}_0\bar{a}\right)^2\nabla^2\right)D_{\bar{z}}=e_{31}\left(1-\bar{l}_m^{\,2}\nabla^2\right)\times\\
&\quad\left[\frac{\partial u_0}{\partial\bar{x}}-\bar{z}\frac{\partial^2 w_0}{\partial\bar{x}^2}+\varphi\left(\frac{\partial^2 w_0}{\partial\bar{x}^2}-\frac{\partial\phi}{\partial\bar{z}}\right)\right]-\\
&\quad k_{33}\left(\beta\sin\left(\beta\bar{z}\right)\bar{\Phi}\left(\bar{x},\bar{t}\right)-E_0\right)
\end{aligned}\tag{24}$$

Based on defined mechanical and electrical relations in Eq. (24), the resultant components can be calculated as follows

$$\begin{aligned}
&N_{\bar{x}\bar{x}}-\left(\bar{e}_0\bar{a}\right)^2\frac{\partial^2 N_{\bar{x}\bar{x}}}{\partial\bar{x}^2}=\left(1-\bar{l}_m^{\,2}\nabla^2\right)\times\\
&\left[\bar{A}_{\bar{x}}\frac{\partial u_0}{\partial\bar{x}}-\bar{B}_{\bar{x}1}\frac{\partial^2 w_0}{\partial\bar{x}^2}+\bar{B}_{\bar{x}2}\left(\frac{\partial^2 w_0}{\partial\bar{x}^2}-\frac{\partial\phi}{\partial\bar{z}}\right)\right]-\\
&\bar{N}^T-\bar{N}^E\\
&M_{\bar{x}\bar{x}}-\left(\bar{e}_0\bar{a}\right)^2\frac{\partial^2 M_{\bar{x}\bar{x}}}{\partial\bar{x}^2}=\left(1-\bar{l}_m^{\,2}\nabla^2\right)\times\\
&\left[\bar{B}_{\bar{x}1}\frac{\partial u_0}{\partial\bar{x}}-\bar{D}_{\bar{x}1}\frac{\partial^2 w_0}{\partial\bar{x}^2}+\bar{D}_{\bar{x}2}\left(\frac{\partial^2 w_0}{\partial\bar{x}^2}-\frac{\partial\phi}{\partial\bar{z}}\right)\right]-\\
&\bar{M}^{T1}-\bar{M}^{E1}
\end{aligned}\tag{25}$$

$$\begin{aligned}
&M^h_{\bar{x}\bar{x}}-\left(\bar{e}_0\bar{a}\right)^2\frac{\partial^2 M^h_{\bar{x}\bar{x}}}{\partial\bar{x}^2}=\left(1-\bar{l}_m^{\,2}\nabla^2\right)\times\\
&\left[\bar{B}_{\bar{x}2}\frac{\partial u_0}{\partial\bar{x}}-\bar{D}_{\bar{x}2}\frac{\partial^2 w_0}{\partial\bar{x}^2}+\bar{D}_{\bar{x}3}\left(\frac{\partial^2 w_0}{\partial\bar{x}^2}-\frac{\partial\phi}{\partial\bar{z}}\right)\right]-\\
&\bar{M}^{T2}-\bar{M}^{E2}\\
&Q_{\bar{x}\bar{z}}-\left(\bar{e}_0\bar{a}\right)^2\frac{\partial^2 Q_{\bar{x}\bar{z}}}{\partial\bar{x}^2}=\left(1-\bar{l}_m^{\,2}\nabla^2\right)\bar{A}_{\bar{x}\bar{z}}\times\\
&\left[\frac{\partial w_0}{\partial\bar{x}}-\phi\right]+\int_A e_{15}\left(\cos\left(\beta\bar{z}\right)\frac{\partial\bar{\Phi}}{\partial\bar{x}}\right)dA\\
&\bar{D}_{\bar{x}}-\left(\bar{e}_0\bar{a}\right)^2\frac{\partial^2\bar{D}_{\bar{x}}}{\partial\bar{x}^2}=\left(1-\bar{l}_m^{\,2}\nabla^2\right)e_{15}\frac{\partial\varphi}{\partial\bar{z}}\times\\
&\left[\frac{\partial w_0}{\partial\bar{x}}-\phi\right]-k_{xx}\left(\cos\left(\beta\bar{z}\right)\frac{\partial\bar{\Phi}}{\partial\bar{x}}\right)\\
&\bar{D}_{\bar{z}}-\left(\bar{e}_0\bar{a}\right)^2\frac{\partial^2\bar{D}_{\bar{z}}}{\partial\bar{x}^2}=\left(1-\bar{l}_m^{\,2}\nabla^2\right)e_{31}\times\\
&\left[\frac{\partial u_0}{\partial\bar{x}}-\bar{z}\frac{\partial^2 w_0}{\partial\bar{x}^2}+\varphi\left(\bar{z}\right)\left(\frac{\partial w_0}{\partial\bar{x}}-\phi\right)\right]-\\
&\alpha\left(\bar{z}\right)\Delta T+k_{\bar{z}\bar{z}}\left(\beta\sin\left(\beta\bar{z}\right)\bar{\Phi}\left(\bar{x},\bar{t}\right)-E_0\right)
\end{aligned}\tag{25}$$

Where superscripts T and E represent thermal and electrical loads. Based on this comments, the force and moment resultants $\bar{N}^T$, $\bar{N}^E$, $\bar{M}^{T1}$, $\bar{M}^{T2}$, $\bar{M}^{E1}$ and $\bar{M}^{E2}$ are expressed as

$$\begin{aligned}
&\begin{pmatrix}\bar{N}^T\\ \bar{N}^E\end{pmatrix}=\int_{-H/2}^{H/2}\begin{pmatrix}E\left(\bar{z}\right)\alpha\left(\bar{z}\right)\Delta T\\ e_{31}\left(\beta\sin\left(\beta\bar{z}\right)\bar{\Phi}\left(\bar{x},\bar{t}\right)-E_0\right)\end{pmatrix}d\bar{z}\\
&\begin{pmatrix}\bar{M}^{T1}\\ \bar{M}^{E1}\end{pmatrix}=\int_{-H/2}^{H/2}\begin{pmatrix}E\left(\bar{z}\right)\alpha\left(\bar{z}\right)\Delta T\\ e_{31}\left(\beta\sin\left(\beta\bar{z}\right)\bar{\Phi}\left(\bar{x},\bar{t}\right)-E_0\right)\end{pmatrix}\bar{z}d\bar{z}\\
&\begin{pmatrix}\bar{M}^{T2}\\ \bar{M}^{E2}\end{pmatrix}=\int_{-H/2}^{H/2}\begin{pmatrix}E\left(\bar{z}\right)\alpha\left(\bar{z}\right)\Delta T\\ e_{31}\left(\beta\sin\left(\beta\bar{z}\right)\bar{\Phi}\left(\bar{x},\bar{t}\right)-E_0\right)\end{pmatrix}\varphi\left(\bar{z}\right)d\bar{z}
\end{aligned}\tag{26}$$

It is noted that, A_x, B_x and D_x in Eq. (25) are the stretching stiffness, stretching-bending coupling stiffness and bending stiffness coefficients , respectively, which can be obtained as

$$\begin{aligned}
&\bar{A}_{\bar{x}}=\int_{-h/2}^{h/2}E\left(\bar{z}\right)dA\\
&\begin{Bmatrix}\bar{B}_{\bar{x}1}\\ \bar{B}_{\bar{x}2}\end{Bmatrix}=\int_{-h/2}^{h/2}\begin{Bmatrix}\bar{z}\\ \varphi\left(\bar{z}\right)\end{Bmatrix}E\left(\bar{z}\right)d\bar{z}\\
&\begin{Bmatrix}\bar{D}_{\bar{x}1}\\ \bar{D}_{\bar{x}2}\\ \bar{D}_{\bar{x}3}\end{Bmatrix}=\int_{-h/2}^{h/2}\begin{Bmatrix}\bar{z}^2\\ \bar{z}\varphi\left(\bar{z}\right)\\ \varphi\left(\bar{z}\right)^2\end{Bmatrix}E\left(\bar{z}\right)d\bar{z}
\end{aligned}\tag{27}$$

To obtain the equations of motion, Eq. (25) should be substituted into Eq. (20). Therefore, four coupled equations

of motion are obtained

$$\begin{aligned}
&\delta u_0 : \left(1-{l_m}^2\nabla^2\right)\times \\
&\left(\bar{A}_{\bar{x}}\frac{\partial^2 u_0}{\partial\bar{x}^2}-\bar{B}_{\bar{x}1}\frac{\partial^3 w_0}{\partial\bar{x}^3}+\bar{B}_{\bar{x}2}\left(\frac{\partial^3 w_0}{\partial\bar{x}^3}-\frac{\partial^2\phi}{\partial\bar{z}^2}\right)\right)+ \\
&\left(1-\left(\bar{e}_0\bar{a}\right)^2\nabla^2\right)F=\left(1-\left(\bar{e}_0\bar{a}\right)^2\nabla^2\right)\times \\
&\left(\bar{I}_A\frac{\partial^2 u_0}{\partial\bar{t}^2}-\bar{I}_{B1}\frac{\partial^3 w_0}{\partial\bar{t}^2\partial\bar{x}}+\bar{I}_{B2}\frac{\partial^3 w_0}{\partial\bar{t}^2\partial\bar{x}}-\bar{I}_{B2}\frac{\partial^2\phi}{\partial\bar{t}^2}\right)
\end{aligned}$$

$$\begin{aligned}
&\delta w_0 : -\left(1-{l_m}^2\nabla^2\right)\times \\
&\left(\bar{B}_{\bar{x}2}\frac{\partial^2 u_0}{\partial\bar{x}^2}-\bar{D}_{\bar{x}2}\frac{\partial^4 w_0}{\partial\bar{x}^4}+\bar{D}_{\bar{x}3}\frac{\partial^4 w_0}{\partial\bar{x}^4}-\bar{D}_{\bar{x}3}\frac{\partial^3\phi}{\partial\bar{x}^3}\right) \\
&+\left(1-{l_m}^2\nabla^2\right)\left(-\bar{D}_{\bar{x}1}\frac{\partial^4 w_0}{\partial\bar{x}^4}+\bar{D}_{\bar{x}2}\frac{\partial^4 w_0}{\partial\bar{x}^4}-\bar{D}_{\bar{x}2}\frac{\partial^3\phi}{\partial\bar{x}^3}\right) \\
&+\bar{M}^{E1}\frac{\partial^2\bar{\Phi}}{\partial\bar{x}^2}-\bar{M}^{E2}\frac{\partial^2\bar{\Phi}}{\partial\bar{x}^2}-\bar{N}^T\frac{\partial^2 w_0}{\partial\bar{x}^2}+\bar{N}^E\frac{\partial^2 w_0}{\partial\bar{x}^2}+ \\
&\bar{N}_0\frac{\partial^2 w_0}{\partial\bar{x}^2}-\bar{K}_w w_0+\bar{K}_s\frac{\partial^2 w_0}{\partial\bar{x}^2}-\bar{C}_d\frac{\partial w_0}{\partial\bar{t}} \\
&+\bar{A}_{\bar{x}\bar{z}}\left(1-{l_m}^2\nabla^2\right)\frac{\partial^2 w_0}{\partial\bar{x}^2}-\bar{A}_{\bar{x}\bar{z}}\left(1-{l_m}^2\nabla^2\right)\frac{\partial\phi}{\partial\bar{x}}+ \\
&E^{15}\frac{\partial^2\bar{\Phi}}{\partial\bar{x}^2}=+\left(1-\left(\bar{e}_0\bar{a}\right)^2\nabla^2\right)\times\left(\bar{I}_{B1}\frac{\partial^3 u_0}{\partial\bar{x}\partial\bar{t}^2}-\right. \\
&\bar{I}_{B2}\frac{\partial^3 u_0}{\partial\bar{x}\partial\bar{t}^2}+\bar{I}_A\frac{\partial^2 w_0}{\partial\bar{t}^2}-\bar{I}_{D1}\frac{\partial^4 w_0}{\partial\bar{t}^2\partial\bar{x}^2}+\bar{I}_{D2}\frac{\partial^4 w_0}{\partial\bar{t}^2\partial\bar{x}^2}+ \\
&\left.\bar{I}_{D2}\frac{\partial^4 w_0}{\partial\bar{t}^2\partial\bar{x}^2}-\bar{I}_{D3}\frac{\partial^4 w_0}{\partial\bar{t}^2\partial\bar{x}^2}-\bar{I}_{D2}\frac{\partial^3\phi}{\partial\bar{x}\partial\bar{t}^2}+\bar{I}_{D3}\frac{\partial^3\phi}{\partial\bar{x}\partial\bar{t}^2}\right)
\end{aligned} \tag{28}$$

$$\begin{aligned}
&\delta\phi : \left(1-{l_m}^2\nabla^2\right)\bar{A}_{\bar{x}\bar{z}}\left(\frac{\partial w_0}{\partial\bar{x}}-\phi\right)+E^{15}\frac{\partial\bar{\Phi}}{\partial\bar{x}}-\left(1-{l_m}^2\nabla^2\right)\times \\
&\left(\bar{B}_{\bar{x}2}\frac{\partial^2 u_0}{\partial\bar{x}^2}-\bar{D}_{\bar{x}2}\frac{\partial^3 w_0}{\partial\bar{x}^3}+\bar{D}_{\bar{x}3}\frac{\partial^3 w_0}{\partial\bar{x}^3}-\bar{D}_{\bar{x}3}\frac{\partial^2\phi}{\partial\bar{x}^2}\right)- \\
&E_3^{13}\frac{\partial\bar{\Phi}}{\partial\bar{x}}=+\left(1-\left(\bar{e}_0\bar{a}\right)^2\nabla^2\right)\times \\
&\left(\bar{I}_{B2}\frac{\partial^2 u_0}{\partial\bar{t}^2}+\bar{I}_{D2}\frac{\partial^3 w_0}{\partial\bar{t}^2\partial\bar{x}}-\bar{I}_{D3}\frac{\partial^3 w_0}{\partial\bar{t}^2\partial\bar{x}}+\bar{I}_{D3}\frac{\partial^2\phi}{\partial\bar{t}^2}\right)
\end{aligned}$$

$$\begin{aligned}
&\delta\bar{\Phi} : \left(1-{l_m}^2\nabla^2\right)\left(E^{15}+E_3^{13}\right)\left(\frac{\partial^2 w_0}{\partial\bar{x}^2}-\frac{\partial\phi}{\partial\bar{x}}\right)-\left(1-{l_m}^2\nabla^2\right)\times \\
&E_2^{31}\frac{\partial^2 w_0}{\partial\bar{x}^2}-k_{xx}\frac{\partial^2\bar{\Phi}}{\partial\bar{x}^2}+k_{zz}\bar{\Phi}=0
\end{aligned}$$

In which, E^{15}, E_2^{31}, E_3^{31}, $k_{\bar{x}\bar{x}}$ and $k_{\bar{z}\bar{z}}$ are calculated as the following form

$$\begin{aligned}
E^{15}&=\int_A e_{15}\frac{\partial\varphi(\bar{z})}{\partial\bar{z}}\cos(\beta\bar{z})\,dA \\
E_2^{31}&=\int_A \beta e_{31}\bar{z}\sin(\beta\bar{z})\,dA \\
E_2^{31}&=\int_A \beta e_{31}\varphi(\bar{z})\sin(\beta\bar{z})\,dA \\
k_{\bar{x}\bar{x}}&=\int_A k_{11}\cos^2(\beta\bar{z})\,dA \\
k_{\bar{z}\bar{z}}&=\int_A k_{33}\beta^2\cos^2(\beta\bar{z})\,dA
\end{aligned} \tag{29}$$

By defining following non-dimensional variables as

$$\begin{aligned}
&E^{15}=\int_A e_{15}\frac{\partial\varphi(\bar{z})}{\partial\bar{z}}\cos(\beta\bar{z})\,dA\,x=\frac{\bar{x}}{L}, \\
&w=\frac{w_0}{h},\ \ \mu_1=\frac{\bar{l}_m}{L},\ \ \mu_2=\frac{\bar{e}_0\bar{a}}{L},\ \ t=\frac{\bar{t}}{T_0}, \\
&T_0=L\sqrt{\frac{\bar{I}_A}{\bar{A}_{\bar{x}}}},\ \ R=\frac{h}{L},\ \ \ A_{xz}=\frac{\bar{A}_{\bar{x}\bar{z}}}{\bar{A}_{\bar{x}}},
\end{aligned} \tag{30}$$

The final dimensionless equations of motion are obtained as

$$\begin{aligned}
&\delta u:\left(1-\mu_1^2\nabla^2\right)\left(\frac{\partial^2 u}{\partial x^2}\right)+\left(1-\mu_2^2\nabla^2\right)F= \\
&\left(1-\mu_2^2\nabla^2\right)\frac{\partial^2 u}{\partial t^2} \\
&\delta w:-\left(1-\mu_1^2\nabla^2\right)\left(-D_{x2}\frac{\partial^4 w}{\partial x^4}+D_{x3}\frac{\partial^4 w}{\partial x^4}-D_{x3}\frac{1}{R}\frac{\partial^3\phi}{\partial x^3}\right)+ \\
&\left(1-\mu_1^2\nabla^2\right)\left(-D_{x1}\frac{\partial^4 w}{\partial x^4}+D_{x2}\frac{\partial^4 w}{\partial x^4}-D_{x2}\frac{1}{R}\frac{\partial^3\phi}{\partial x^3}\right) \\
&+M^{E1}\frac{\partial^2\Phi}{\partial x^2}-M^{E2}\frac{\partial^2\Phi}{\partial x^2}-N^T\frac{\partial^2 w}{\partial x^2}+N^E\frac{\partial^2 w}{\partial x^2}-K_w w \\
&+K_s\frac{\partial^2 w}{\partial x^2}-C_d\frac{\partial w}{\partial t}+A_{xz}\left(1-\mu_1^2\nabla^2\right)\frac{\partial^2 w}{\partial x^2} \\
&-A_{xz}\left(1-\mu_1^2\nabla^2\right)\frac{1}{R}\frac{\partial\phi}{\partial\bar{x}}+E^{15}\frac{\partial^2\Phi}{\partial\bar{x}^2}=\left(1-\mu_2^2\nabla^2\right)\left(\frac{\partial^2 w}{\partial t^2}\right. \\
&-I_{D1}\frac{\partial^4 w_0}{\partial\bar{t}^2\partial\bar{x}^2}+2I_{D2}\frac{\partial^4 w}{\partial t^2\partial x^2}-I_{D3}\frac{\partial^4 w}{\partial t^2\partial x^2}-I_{D2}\frac{1}{R}\frac{\partial^3\phi}{\partial x\partial t^2} \\
&\left.+I_{D3}\frac{1}{R}\frac{\partial^3\phi}{\partial x\partial t^2}\right) \\
&\delta\phi:\left(1-\mu_1^2\nabla^2\right)A_{xz}\left(\frac{\partial w}{\partial x}-\phi\right)+E^{15}\frac{\partial\Phi}{\partial x}-\left(1-\mu_1^2\nabla^2\right)\times \\
&\left(-D_{x2}\frac{\partial^3 w}{\partial x^3}+D_{x3}\frac{\partial^3 w}{\partial x^3}-D_{x3}\frac{1}{R}\frac{\partial^2\phi}{\partial x^2}\right)-E_3^{13}\frac{\partial\Phi}{\partial x}= \\
&+\left(1-\mu_2^2\nabla^2\right)\left(I_{D2}\frac{\partial^3 w}{\partial t^2\partial x}-I_{D3}\frac{\partial^3 w}{\partial t^2\partial x}+I_{D3}\frac{\partial^2\phi}{\partial t^2}\right)
\end{aligned} \tag{31}$$

$$\delta\Phi:\left(1-\mu_1{}^2\nabla^2\right)\left(E^{15}+E_3{}^{13}\right)\left(\frac{\partial^2 w}{\partial x^2}-\frac{1}{R}\frac{\partial\phi}{\partial x}\right)-$$
$$\left(1-\mu_1{}^2\nabla^2\right)E_2^{31}\frac{\partial^2 w}{\partial x^2}-k_{xx}\frac{\partial^2\Phi}{\partial x^2}+k_{zz}\frac{1}{R^2}\Phi=0 \tag{31}$$

Boundary conditions to solve Eq. (31) are defined as (Ansari *et al*. 2014a, Ait Amar Meziane *et al*. 2014)

$$\begin{aligned} &u=w=\phi=\Phi=0 \qquad \textit{for clamped ends}\\ &u=w=\frac{\partial\phi}{\partial x}=\Phi=0 \qquad \textit{for hinged ends}\end{aligned} \tag{32}$$

4. Non-linear vibration analysis

In order to solve DIR equations of motion, DQ method is employed. Based on the aforementioned method, the approximate solution of a function $f(x)$ can be found in the form

$$f\left(x\right)=\sum_{j=1}^{N}\lambda_j\psi_j\left(x\right) \tag{33}$$

Where, N is the total number of grid points, inside a closed interval. In this method, the smooth basis functions are selected as the various functions form such as Chebyshev polynomials, Exponential polynomials, and Fourier polynomials (Tornabene *et al*. 2014a, b). Also, the Eq. (33) for the one-dimensional case can be written in matrix form as

$$f=C\lambda \tag{34}$$

In which, $f=[f(x_1),f(x_2),f(x_3),\ldots,f(x_N)]^T$ is the vector of the unknown function values, λ is the vector of the unknown coefficients λ_j and the components of the coefficient matrix C are given by $C_{ij}=\psi_j(x_i)$ for $i,j=1.2.3,\ldots,N$ (Tornabene *et al*. 2014a). Since the n'th order derivative of the Eq. (33) can be computed, the derivative is directly transferred to the functions $\psi_j(x)$, because the unknown coefficients λ_j do not depend on the variable x (Tornabene *et al*. 2014b)

$$\frac{d^n f\left(x\right)}{dx^n}=\sum_{j=1}^{N}\lambda_j\frac{d^n\psi_j\left(x\right)}{dx^n},\ n=1,2,3,..,N-1 \tag{35}$$

Eq. (35) is rewritten as following matrix form

$$\begin{aligned} &f^{(n)}=C^{(n)}\lambda\ \ with\ C_{ij}^{(n)}=\left.\frac{d^n\psi_j\left(x\right)}{dx^n}\right|_{x_i}=\psi_j^{(n)}\left(x\right)\\ &\Rightarrow\ for\ i,j=1,2,3,...,N\end{aligned} \tag{36}$$

Therefore, the governing equations and boundary conditions are discretized by means of aforementioned method (Ghorbanpour Arani *et al*. 2012a, b). In this investigation, the cosine pattern is employed to generate the DQ point system as the following form

$$x_j=\frac{1}{2}\left\{1-\cos\left(\frac{\pi(j-1)}{N-1}\right)\right\},\qquad j=1,2,.....,N \tag{37}$$

In addition, column vectors for variables u, w, ϕ and Φ are considered as follows

$$\begin{aligned} &u=\left[u_1\ \ u_2\ \ ...\ \ u_N\right],\quad w=\left[w_1\ \ w_2\ \ ...\ \ w_N\right],\\ &\phi=\left[\phi_1\ \ \phi_2\ \ ...\ \ \phi_N\right],\quad \Phi=\left[\Phi_1\ \ \Phi_2\ \ ...\ \ \Phi_N\right],\end{aligned} \tag{38}$$

To solve Eq. (31) and associated boundary conditions Eq. (32) for DIR analysis of the sandwich piezoelectric nano-beam by DQ method, the weighting coefficients for the second, third and fourth derivatives with attention to Eq. (36) are determined as the following form

$$\left.\frac{\partial^r f\left(\varsigma,\lambda\right)}{\partial\varsigma^r}\right|_{(\varsigma,\lambda)=(\varsigma_j,\lambda_j)}=\sum_{j=1}^{N_\varsigma}C_{ij}^{\varsigma(r)}f\left(\varsigma_j,\lambda_m\right)=$$
$$\sum_{j=1}^{N_\varsigma}C_{ij}^{\varsigma(r)}f_{jm},\begin{cases}i=1,2,...,N_\varsigma\\ m=1,2,...,N_\lambda\\ r=1,2,...,N_\varsigma-1\end{cases} \tag{39}$$

In which weighting coefficients C_{ij}^{ζ} are expressed as

$$\left.\frac{\partial^r f\left(\varsigma,\lambda\right)}{\partial\varsigma^r}\right|_{(\varsigma,\lambda)=(\varsigma_j,\lambda_j)}=\sum_{j=1}^{N_\varsigma}C_{ij}^{\varsigma(r)}f\left(\varsigma_j,\lambda_m\right)=$$
$$\sum_{j=1}^{N_\varsigma}C_{ij}^{\varsigma(r)}f_{jm},\begin{cases}i=1,2,...,N_\varsigma\\ m=1,2,...,N_\lambda\\ r=1,2,...,N_\varsigma-1\end{cases}$$
$$C_{ij}^{\varsigma}=\begin{cases}\dfrac{M\left(\varsigma_i\right)}{\left(\varsigma_i-\varsigma_j\right)M\left(\varsigma_j\right)} & for\quad i\neq j\\ -\displaystyle\sum_{\substack{j=1\\ i\neq j}}^{N_\varsigma}C_{ij}^{\varsigma} & for\quad i=j\end{cases} \tag{40}$$

It is noted that in Eq. (40), $M(\varsigma_i)$ is represented as following form

$$M\left(\varsigma_i\right)=\prod_{\substack{j=1\\ i\neq j}}^{N_\varsigma}\left(\varsigma_i-\varsigma_j\right) \tag{41}$$

The weighting coefficients for various derivatives such as the second, third and fourth derivatives are defined as

$$\begin{aligned} &M\left(\varsigma_i\right)=\prod_{\substack{j=1\\ i\neq j}}^{N_\varsigma}\left(\varsigma_i-\varsigma_j\right)\\ &C_{ij}^{\varsigma(2)}=\sum_{k=1}^{N_\varsigma}C_{ik}^{\varsigma(1)}C_{kj}^{\varsigma(1)},\\ &C_{ij}^{\varsigma(3)}=\sum_{k=1}^{N_\varsigma}C_{ik}^{\varsigma(1)}C_{kj}^{\varsigma(2)}=\sum_{k=1}^{N_\varsigma}C_{ik}^{\varsigma(2)}C_{kj}^{\varsigma(1)},\\ &C_{ij}^{\varsigma(4)}=\sum_{k=1}^{N_\varsigma}C_{ik}^{\varsigma(1)}C_{kj}^{\varsigma(3)}=\sum_{k=1}^{N_\varsigma}C_{ik}^{\varsigma(3)}C_{kj}^{\varsigma(1)}\end{aligned} \tag{42}$$

Applying the Eqs. (39) and (40) to Eq. (31), one can obtain a set of linear ordinary differential equations as

$$\begin{aligned}
&\delta u: \sum_{m=1}^{N} C_{im}^{(2)} u_m - \mu_1{}^2 \sum_{m=1}^{N} C_{im}^{(4)} u_m = \frac{\partial^2 u}{\partial t^2} - \\
&\mu_2{}^2 \sum_{m=1}^{N} C_{im}^{(2)} \frac{\partial^2 u}{\partial t^2} \\
&\delta w: \left(D_{x2} \sum_{m=1}^{N} C_{im}^{(4)} w_m - D_{x3} \sum_{m=1}^{N} C_{im}^{(4)} w_m + D_{x3} \frac{1}{R} \sum_{m=1}^{N} C_{im}^{(3)} \phi_m \right) \\
&+ \mu_1{}^2 \left(-D_{x2} \sum_{m=1}^{N} C_{im}^{(6)} w_m + D_{x3} \sum_{m=1}^{N} C_{im}^{(6)} w_m - D_{x3} \frac{1}{R} \sum_{m=1}^{N} C_{im}^{(5)} \phi_m \right) \\
&+ \left(-D_{x1} \sum_{m=1}^{N} C_{im}^{(4)} w_m + D_{x2} \sum_{m=1}^{N} C_{im}^{(4)} w_m - D_{x2} \frac{1}{R} \sum_{m=1}^{N} C_{im}^{(3)} \phi_m \right) + \\
&\mu_1{}^2 \left(+D_{x1} \sum_{m=1}^{N} C_{im}^{(6)} w_m - D_{x2} \sum_{m=1}^{N} C_{im}^{(6)} w_m + D_{x2} \frac{1}{R} \sum_{m=1}^{N} C_{im}^{(5)} \phi_m \right) \\
&+ M^{E1} \sum_{m=1}^{N} C_{im}^{(2)} \Phi_m - M^{E2} \sum_{m=1}^{N} C_{im}^{(2)} \Phi_m - N^T \sum_{m=1}^{N} C_{im}^{(2)} w_m + \\
&N^E \sum_{m=1}^{N} C_{im}^{(2)} w_m - K_w w_m + K_s \sum_{m=1}^{N} C_{im}^{(2)} w_m - C_d \frac{\partial w_m}{\partial t} + \\
&A_{xz} \sum_{m=1}^{N} C_{im}^{(2)} w_m - A_{xz} \mu_1{}^2 \sum_{m=1}^{N} C_{im}^{(2)} w_m - A_{xz} \frac{1}{R} \sum_{m=1}^{N} C_{im}^{(1)} w_m \\
&+ A_{xz} \frac{\mu_1{}^2}{R} \sum_{m=1}^{N} C_{im}^{(3)} w_m + E^{15} \sum_{m=1}^{N} C_{im}^{(2)} \Phi_m = \left(\frac{\partial^2 w}{\partial t^2} - \right. \\
&I_{D1} \sum_{m=1}^{N} C_{im}^{(2)} \frac{\partial^2 w}{\partial t^2} + 2 I_{D2} \sum_{m=1}^{N} C_{im}^{(2)} \frac{\partial^2 w}{\partial t^2} - I_{D3} \sum_{m=1}^{N} C_{im}^{(2)} \frac{\partial^2 w}{\partial t^2} \\
&\left. - I_{D2} \frac{1}{R} \sum_{m=1}^{N} C_{im}^{(1)} \frac{\partial^2 \phi}{\partial t^2} + I_{D3} \frac{1}{R} \sum_{m=1}^{N} C_{im}^{(1)} \frac{\partial^2 \phi}{\partial t^2} \right) \\
&- \mu_2{}^2 \left(\frac{\partial^2 w}{\partial t^2} - I_{D1} \sum_{m=1}^{N} C_{im}^{(4)} \frac{\partial^2 w}{\partial t^2} + 2 I_{D2} \sum_{m=1}^{N} C_{im}^{(4)} \frac{\partial^2 w}{\partial t^2} \right. \\
&- I_{D3} \sum_{m=1}^{N} C_{im}^{(4)} \frac{\partial^2 w}{\partial t^2} - I_{D2} \frac{1}{R} \sum_{m=1}^{N} C_{im}^{(3)} \frac{\partial^2 \phi}{\partial t^2} + \\
&\left. I_{D3} \frac{1}{R} \sum_{m=1}^{N} C_{im}^{(3)} \frac{\partial^2 \phi}{\partial t^2} \right) \\
&\delta \phi: A_{xz} \left(\sum_{m=1}^{N} C_{im}^{(1)} w_m - \phi_m \right) - \mu_1{}^2 \left(\sum_{m=1}^{N} C_{im}^{(3)} w_m - \sum_{m=1}^{N} C_{im}^{(3)} \phi_m \right) \\
&+ E^{15} \sum_{m=1}^{N} C_{im}^{(1)} \Phi_m + \left(D_{x2} \sum_{m=1}^{N} C_{im}^{(3)} w_m - D_{x3} \sum_{m=1}^{N} C_{im}^{(3)} w_m + \right. \\
&\left. D_{x3} \frac{1}{R} \sum_{m=1}^{N} C_{im}^{(2)} \phi_m \right) + \mu_1{}^2 \left(-D_{x2} \sum_{m=1}^{N} C_{im}^{(5)} w_m + D_{x3} \sum_{m=1}^{N} C_{im}^{(5)} w_m \right. \\
&\left. - D_{x3} \frac{1}{R} \sum_{m=1}^{N} C_{im}^{(4)} \phi_m \right) - E_3{}^{13} \sum_{m=1}^{N} C_{im}^{(1)} \Phi_m = \\
&\left(I_{D2} \sum_{m=1}^{N} C_{im}^{(1)} \frac{\partial^2 w_m}{\partial t^2} - I_{D3} \sum_{m=1}^{N} C_{im}^{(1)} \frac{\partial^2 w_m}{\partial t^2} + I_{D3} \frac{\partial^2 \phi_m}{\partial t^2} \right) \\
&- \mu_2{}^2 \left(I_{D2} \sum_{m=1}^{N} C_{im}^{(3)} \frac{\partial^2 w_m}{\partial t^2} - I_{D3} \sum_{m=1}^{N} C_{im}^{(3)} \frac{\partial^2 w_m}{\partial t^2} + I_{D3} \frac{\partial^2 \phi_m}{\partial t^2} \right) \\
&\delta \Phi: E^{15} \sum_{m=1}^{N} C_{im}^{(2)} w_m - E^{15} \frac{1}{R} \sum_{m=1}^{N} C_{im}^{(1)} \phi_m - \mu_1{}^2 E^{15} \sum_{m=1}^{N} C_{im}^{(4)} w_m + \\
&\mu_1{}^2 E^{15} \frac{1}{R} \sum_{m=1}^{N} C_{im}^{(3)} \phi_m + E_3{}^{13} \sum_{m=1}^{N} C_{im}^{(2)} w_m - E_3{}^{13} \frac{1}{R} \sum_{m=1}^{N} C_{im}^{(1)} \phi_m - \\
&\mu_1{}^2 E_3{}^{13} \sum_{m=1}^{N} C_{im}^{(4)} w_m + \mu_1{}^2 E_3{}^{13} \frac{1}{R} \sum_{m=1}^{N} C_{im}^{(3)} \phi_m - E_2^{31} \sum_{m=1}^{N} C_{im}^{(2)} w_m \\
&+ \mu_1{}^2 E_2^{31} \sum_{m=1}^{N} C_{im}^{(4)} w_m - k_{xx} \sum_{m=1}^{N} C_{im}^{(4)} \Phi_m + k_{zz} \frac{1}{R^2} \Phi_m = 0
\end{aligned} \tag{43}$$

The boundary conditions of the sandwich nano-beam using DQ method are expressed as

$$\begin{cases} u_1 = w_1 = \phi_1 = \Phi_1 = 0 \\ u_N = w_N = \phi_N = \Phi_N = 0 \end{cases} \Rightarrow \textit{clamped ends}$$

$$\begin{cases} u_1 = w_1 = \sum_{m=1}^{N} C_{1m}^{(1)} \phi_m = \Phi_1 = 0 \\ u_N = w_N = \sum_{m=1}^{N} C_{Nm}^{(1)} \phi_m = \Phi_N = 0 \end{cases} \Rightarrow \textit{hinged ends} \tag{44}$$

The discretized forms of the governing equations can be expressed as

$$M\ddot{d} + C\dot{d} + \left(K - PK_G \right) d = 0 \tag{45}$$

Where M, C, and K are the mass, damping, and stiffness matrices, respectively, K_G is the geometrical stiffness matrix, d is the displacement vector (i.e., $d = [u, v, w]$), and

$$P(t) = \alpha P_{Cr} + \beta P_{Cr} \cos(\omega t) \tag{46}$$

In which ω is the frequency of excitation, P_{cr} is the static buckling load, α and β may be defined as static and dynamic load factors, respectively

5. Bolotin method

In order to determine the DIR of piezoelectric sandwich nano-beam, the method suggested by Bolotin (Maraghi et al. 2013) is used. Hence, the component of d can be written in the Fourier series with the period 2T as

$$d = \sum_{k=1,2,3,\ldots}^{+\infty} \left(a_k \sin \frac{k\omega t}{2} + b_k \cos \frac{k\omega t}{2} \right) \tag{47}$$

Where a_k and b_k are undetermined constants according to this method. Regarding to aforementioned method, the first instability region is usually the most important in studies of structures. It is due to the fact that the first DIR is wider than other DIRs, and the structural damping in higher regions becomes neutralized (Maraghi *et al*. 2013). Substituting Eq. (47) into Eq. (45) and setting the coefficients of each sine and cosine as well as the sum of the constant terms to zero, yield

$$\left| K - P_{Cr} \alpha K_G \pm P_{Cr} \frac{\beta}{2} K_G \mp C \frac{\omega}{2} - M \frac{\omega^2}{4} \right| = 0 \tag{48}$$

Table 1 The material and geometrical properties of the constituent material of the sandwich piezoelectric nano-beam (Ke *et al*. 2010, Rafiee *et al*. 2013, Arefi and Zenkour 2017a-i)

Materials	Density ($\frac{kg}{m^3}$)	Young's moduli (GPa)	Heat expansion coefficient ($1/C^o$)	$e_{31}(C/m^2)$	$e_{15}(C/m^2)$	$k_{11}(C/Vm)$	$k_{33}(C/Vm)$
Piezoelectric	5.55×10^3	226	0.9×10^{-6}	-2.2	5.8	5.64×10^{-9}	6.35×10^{-9}
CNT	1400	5.6×10^3	3.4584×10^{-6}				

Solving the above equation based on the eigenvalue problem, the variation of ω with respect to α can be plotted as the DIR.

6. Numerical results and discussion

A comparison is carried out to verify the reliability of the present formulation and solution methodology. In this section, numerical results are presented for the DIR of the sandwich piezoelectric nano-beam with FG-CNTRC face-sheets including different HOSDBTs embedded in Visco-elastic-Pasternak environment subjected to external constant voltage and change temperature. The material properties and geometrical specifications of the sandwich piezoelectric nano-beam are presented in Table 1. To justify the accuracy of the present study, a comparison with existing references based on Timoshenko beam theory is presented. It is necessary noted that in this comparison thickness of the core are equal to zero and CNTs aligned as uniform pattern along to height of the beam. Fig. 3 shows comparison between the obtained results in present study and results achieved by Ke *et al*. (2010) in Reference. Regarding to these comparisons it is deduced that the current extracted formulations have the acceptable accuracy and precision. Fig. 3 presents the numerical results of the natural frequency of a beam as a function of L/h ratio. According to data presented in Fig. 3, the numerical results of current method are in good agreement with literature.

Fig. 4 shows variation of dynamic load factor of sandwich piezoelectric nano-beam with FG -CNTRC face-sheets in terms of the frequency of dynamic excitation for various Visco-Winkler and Pasternak coefficients of foundation. According to the presented results in this figure can be concluded that with increasing viscosity, spring and shearing coefficients of the foundation DIR shifts to right as frequency of dynamic excitation for instability of the beam to increase. Also enhancing the mentioned parameters causes the DIR of the sandwich piezoelectric nano-beam becomes narrower that this makes the system more stable and also instability occur in less excitation frequency range. This is due to the fact that increasing the mentioned parameters causes the stiffness of the beam to increase.

The effects of $\frac{L}{h}$ ratio on the DIR are investigated and the obtained results presented in Fig. 5. Regarding to these results can be concluded that increasing the $\frac{L}{h}$ ratio leads to the DIR becomes wider and shifts to lefts. Therefore it can be deduced that the increase in $\frac{L}{h}$ ratio causes the sandwich piezoelectric becomes more instable. Therefore this makes

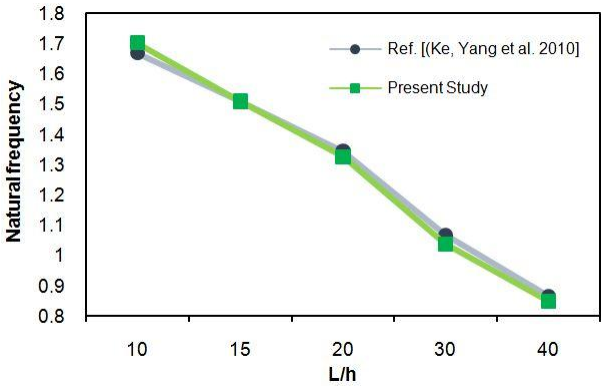

Fig. 3 The comparison between obtained results in present work and results yielded in Ref (Ke *et al*. 2010)

the instability to occur at low frequencies and DIR become wider. Also, with wider range of instability, the frequencies that fall within the range of instability are more.

The influences of various HOSDBTs on the DIR of the sandwich piezoelectric nano-beam are studied and achieved results represented in Fig. 6. With attention to these results can be deduced that FSDBT has more stability with respect to other HOSDBTs. Therefore it can be said that this theory (FSDBT) provides more stiffness for the sandwich piezoelectric nano-beam.

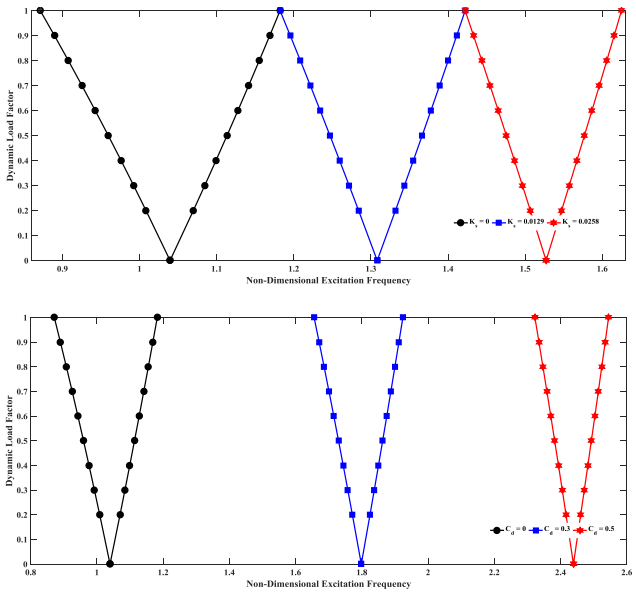

Fig. 4 The effects of the Pasternak foundation coefficients on DIR

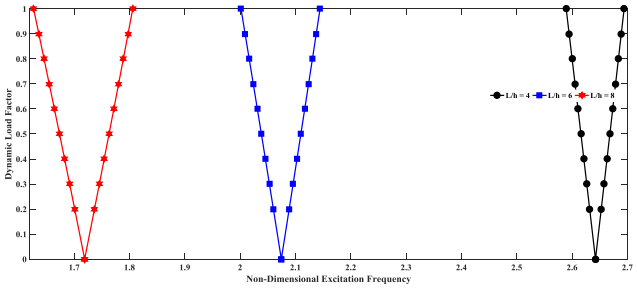

Fig. 5 The effects of the $\frac{L}{h}$ ratio on DIR

Fig. 7 presented the effects of small scale parameters on the DIR of the sandwich piezoelectric nano-beam. According to these results can be concluded that increasing the nonlocal and strain gradient parameters lead to shift the DIR to left and right as this cause decrease and increase the stability of the sandwich nano-beam, respectively. Also enhancing the nonlocal and strain gradient parameter cause the DIR becomes wider and narrower.

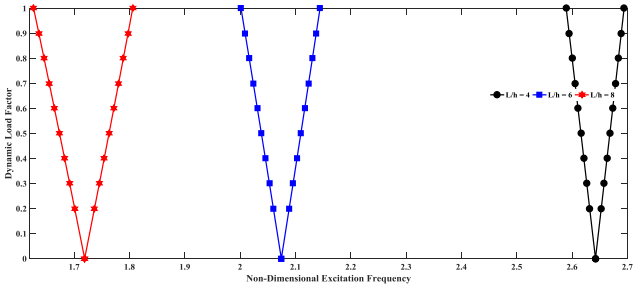

Fig. 6 The effects of various HOSDBTs on DIR of the sandwich piezoelectric nano-beam

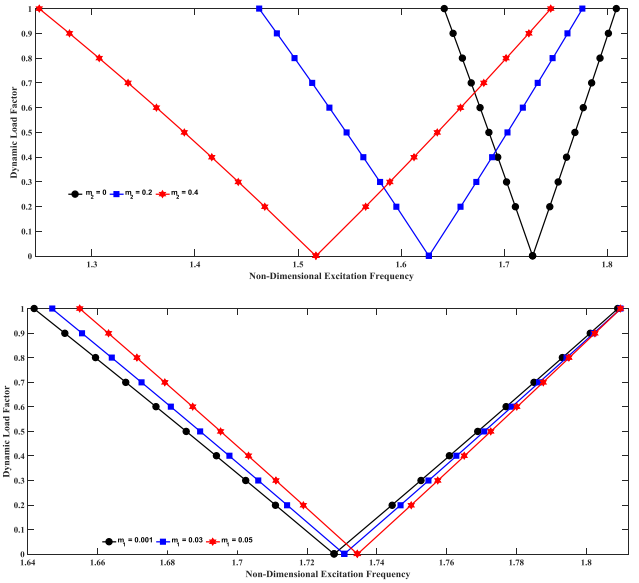

Fig. 7 The effects of nonlocal parameter and strain gradient parameter on DIR of the sandwich piezoelectric nano-beam

In Fig. 8, the effects of the volume fraction of the CNTs (V_{CNT}) on the DIR of sandwich piezoelectric nano-beam are investigated. Regarding to these results can be deduced that enhancing the volume fraction of the CNTs in top and bottom face-sheets leads to shift DIR to right therefore this causes the instability to occur at high frequencies and DIR become narrower. Also, with narrower range of instability, the frequencies that fall within the range of instability are less.

The dynamic load factor of the sandwich piezoelectric nano-beam versus to non-dimensional excitation frequency is calculated for various $\frac{h_f}{h_H}$ ratio and these results are presented in Fig. 9. According to aforementioned results, it can be concluded that increasing $\frac{h_f}{h_H}$ ratio leads to decrease of non-dimensional excitation frequency and therefore instability is occurred in low frequency. In other hand with attention to obtained results can be concluded that DIR becomes wider by increasing $\frac{h_f}{h_H}$ ratio.

The influences of the various distributions of the CNTs in face-sheets on the DIR of sandwich piezoelectric nano-beam are investigated and achieved results represented in Fig. 10. Regarding to aforementioned results can be deduced that DIR is occurred in high frequencies for VA pattern and in low frequency for AV pattern.

The effects of the applied voltage and temperature change on the DIR of the sandwich piezoelectric nano-beam are showed in Fig. 11. According to these results, increasing the temperature change and applied voltage cause the DIR shift to left as instability occur in low frequencies. Also

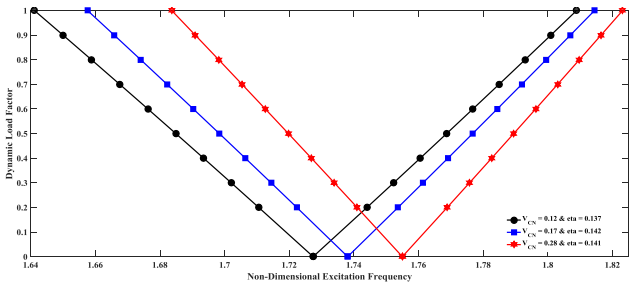

Fig. 8 The effects of various volume fraction of CNTs on DIR of the sandwich piezoelectric nano-beam

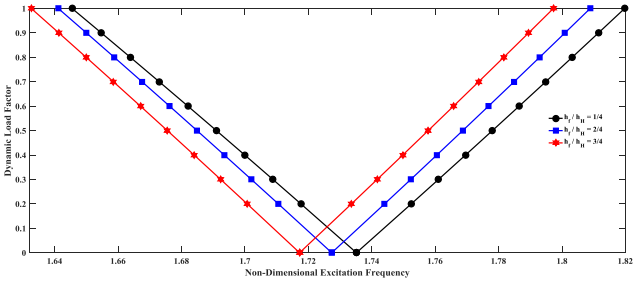

Fig. 9 The effects of various $\frac{h_f}{h_H}$ on DIR of the sandwich piezoelectric nano-beam

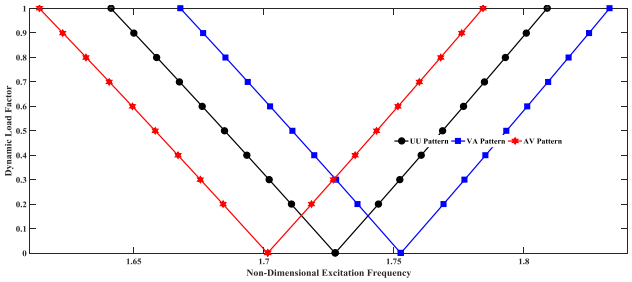

Fig. 10 The effects of various patterns of CNTs in face-sheets on DIR of the sandwich piezoelectric nano-beam

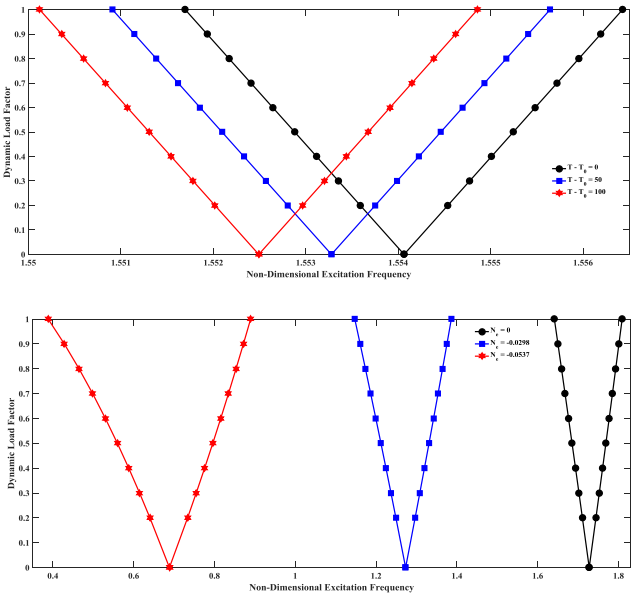

Fig. 11 The effects of applied voltage and temperature change on DIR of the sandwich piezoelectric nano-beam

enhancing of the applied voltage leads to the DIR become wider and therefore instability occurs in a greater range of excitation frequencies.

7. Conclusions

Analysis of the DIR of the sandwich piezoelectric nano-beams with FG-CNTRC face-sheets was implemented in this investigation. Various HOSDBTs were employed to investigate DIR of the piezoelectric sandwich nano-beams with FG-CNTRC face-sheets. Also the applied constant voltage and also the nonlocal strain gradient theory to involve the nonlocal and strain gradient parameters were considered in deriving the equations of motion. Then, the governing equations were solved by the DQM and the dynamic laud factor versus non-dimensional excitation frequencies for DIR was obtained. The effects of some parameters such as various shear deformation theories, nonlocal parameter, the volume fraction of the CNTs, various distributions of the CNTs, the ratio of the face-sheets thickness to core thickness and other important parameters in designing and controlling the DIR were studied in detail. The most important results of this study are presented as:

(1) The nonlocal parameters (ea_0) and the strain gradient parameter (l_m) have significant effects on the DIR of the sandwich piezoelectric nano-beam with FG-CNTRC face sheets. It is observed that enhancing aforementioned parameters leads to shift the DIR to left and right, respectively as instability occur in low and high excitation frequencies.

(2) With attention to results, can be deduced that various HOSDBTs have the important effects on the DIR analysis. Also it can be concluded that among the various HOSDBTs, FSDBT has larger excitation frequencies of the DIR with respect to other HOSDBTs.

(3) Investigation on the effect of the Visco-elastic-Pasternak foundation parameters on the DIR of the sandwich piezoelectric nano-beam leads to important conclusions. Increasing the Winkler (K_w), damping (C_d) and shearing (K_s) coefficients caused that the excitation frequencies increases as DIR occur in larger excitation frequencies. Also it is noted that enhancing aforementioned parameters leads to DIR becomes narrower range. In addition the applied constant voltage and temperature change has important influences on DIR of the sandwich piezoelectric nano-beam as increasing the mentioned parameters leads to decreasing excitation frequencies for instability and instability occurs in a wider range of excitation frequencies.

(4) Volume fraction of the CNTs in face-sheets can strongly change the non-dimensional excitation frequencies for DIR of sandwich piezoelectric nano-beam. The numerical results indicate that DIR for different HOSDBTs shift to right with increasing the volume fraction of CNTs in face-sheets. Also it is deduced that enhancing the volume fraction of CNTs causes DIR occur in a narrower range of the excitation frequencies and also VA pattern is more stable with respect to other distribution pattern.

References

Ait Amar Meziane, M., Abdelaziz, H.H. and Tounsi, A. (2014), "An efficient and simple refined theory for buckling and free vibration of exponentially graded sandwich plates under various boundary conditions", *J. Sandw. Struct. Mater.*, **16**(3), 293-318.

Amine, Z., Houari, M.S.A., Bousahla, A.A. and Tounsi, A. (2015), "A mechanical response of functionally graded nanoscale beam: an assessment of a refined nonlocal shear deformation theory beam theory", *Struct. Eng. Mech., Int. J.*, **54**(4), 693-710.

Ansari, R., Faghih Shojaei, M., Mohammadi, V., Gholami, R. and Sadeghi, S. (2014a), "Nonlinear forced vibration analysis of functionally graded carbon nanotube-reinforced composite Timoshenko beams", *Compos. Struct.*, **113**, 316-327.

Ansari, R., Shojaei, M.F., Mohammadi, V., Gholami, R. and Darabi, M.A. (2014b), "Nonlinear vibrations of functionally graded mindlin microplates based on the modified couple stress theory", *Compos. Struct.*, **114**, 124-134.

Ansari, R., Mohammadi, V., Faghih Shojaei, M., Gholami, R. and Sahmani, S. (2014c), "On the forced vibration analysis of Timoshenko nanobeams based on the surface stress elasticity theory", *Compos. Part B*: *Eng*., **60**, 158-166.

Arefi, M. (2016), "Analysis of wave in a functionally graded magneto-electro-elastic nano-rod using nonlocal elasticity model subjected to electric and magnetic potentials", *Acta Mech*., **227**, 2529-2542.

Arefi, M. and Allam, M.N.M. (2015), "Nonlinear responses of an arbitrary FGP circular plate resting on the Winkler-Pasternak foundation", *Smart. Struct. Syst., Int. J*., **16**(1), 81-100.

Arefi, M. and Zenkour, A.M. (2017a), "Transient analysis of a three-layer microbeam subjected to electric potential", *Int. J. Smart. Nano. Mater*., **8**(1), 20-40.

Arefi, M. and Zenkour, A.M. (2017b), "Size-dependent free vibration and dynamic analyses of piezo-electro-magnetic sandwich nanoplates resting on viscoelastic foundation", *Phys B*: *Cond. Matt*., **521**, 188-197.

Arefi, M. and Zenkour, A.M. (2017c), "Electro-magneto-elastic analysis of a three-layer curved beam", *Smart Struct. Syst*., *Int. J*., **19**(6), 695-703.

Arefi, M. and Zenkour, A.M. (2017d), "Influence of magneto-electric environments on size-dependent bending results of three-layer piezomagnetic curved nanobeam based on sinusoidal shear deformation theory", *J. Sandw. Struct. Mater*. DOI: 1099636217723186

Arefi, M. and Zenkour, A.M. (2017e), "Effect of thermo-magneto-electro-mechanical fields on the bending behaviors of a three-layered nanoplate based on sinusoidal shear-deformation plate theory", *J. Sandw. Struct. Mater*. DOI: 1099636217697497

Arefi, M. and Zenkour, A.M. (2017f), "Size dependent vibration and bending analyses of the piezomagnetic three-layer nanobeams", *Appl. Phys. A, Mater. Sci. Processing*.

Arefi, M. and Zenkour, A.M. (2017g), "Thermo-electro-mechanical bending behavior of sandwich nanoplate integrated with piezoelectric face-sheets based on trigonometric plate theory", *Compos. Struct*., **162**, 108-122.

Arefi, M. and Zenkour, A.M. (2017h), "Transient sinusoidal shear deformation formulation of a size-dependent three-layer piezo-magnetic curved nanobeam", *Acta. Mech*., **228**(10), 3657-3674.

Arefi, M. and Zenkour, A.M. (2017i), "Vibration and bending analysis of a sandwich microbeam with two integrated piezo-magnetic face-sheets", *Compos. Struct*., **159**, 479-490.

Arefi, M. and Zenkour, A.M. (2017j), "Wave propagation analysis of a functionally graded magneto-electro-elastic nanobeam rest on Visco-Pasternak foundation", *Mech. Res. Commun*., **79**, 51-62.

Arefi, M. and Zenkour, A.M. (2018), "Employing the coupled stress components and surface elasticity for nonlocal solution of wave propagation of a functionally graded piezoelectric Love nanorod model", *J. Intel. Mater. Syst. Struct*., **28**(17), 2403-2413.

Arefi, M., Pourjamshidian, M. and Ghorbanpour Arani, A. (2017), "Application of nonlocal strain gradient theory and various shear deformation theories to nonlinear vibration analysis of sandwich nano-beam with FG-CNTRCs face-sheets in electro-thermal environment", *Appl. Phys. A*, **123**, 323.

Arefi, M. Zamani, M.H. and Kiani, M. (2018), "Size-dependent free vibration analysis of three-layered exponentially graded nanoplate with piezomagnetic face-sheets resting on Pasternak's foundation", *J. Intel. Mater. Syst. Struct*., **29**(5), 774-786.

Arvin, H. and Bakhtiari-Nejad, F. (2013), "Nonlinear free vibration analysis of rotating composite Timoshenko beams", *Compos. Struct*., **96**, 29-43.

Ashrafi, B. and Hubert, P. (2006), "Vengallatore S. Carbon nanotube-reinforced composites as structural materials for microactuators in microelectromechanical systems", *Nanotechnol*., **17**, 4895-4903.

Bennoun, M., Sid Ahmed Houari, M. and Tounsi, A. (2016), "A novel five variable refined plate theory for vibration analysis of functionally graded sandwich plates", *Mech. Adv. Mater. Struct*., **23**(4), 423-431.

Boukhari, A., Hassen, A.A., Tounsi, A. and Hassan, S. (2016), "An efficient shear deformation theory for wave propagation of functionally graded material plates", *Struct. Eng. Mech., Int. J*., **57**(5), 837-859.

Bousahla, A.A., Benyoucef, S., Tounsi, A. and Hassan, S. (2016), "On thermal stability of plates with functionally graded coefficient of thermal expansion", *Struct. Eng. Mech., Int. J*., **60**(2), 313-335.

Chen, L.-W., Lin, C.-Y. and Wang, C.-C. (2002), "Dynamic stability analysis and control of a composite beam with piezoelectric layers", *Compos. Struct*., **56**, 97-109.

Ebrahimy, F. and Hosseini, S.-H. (2016), "Nonlinear electroelastic vibration analysis of NEMS consisting of double-viscoelastic nanoplates", *Appl. Phys. A*, **122**(10), 922.

El-Haina, F., Bakora, A., Anis Bousahla, A. and Tounsi, A. (2017), "A simple analytical approach for thermal buckling of thick functionally graded sandwich plates", *Struct. Eng. Mech., Int. J*., **63**(5), 585-595.

Eringen, A.C. (1983), "On differential equations of nonlocal elasticity and solutions of screw dislocation and surface waves", *J. Appl. Phys*., **54**(9), 4703-4710.

Esawi, A. and Farag, M. (2007), "Carbon nanotube reinforced composites: potential and current challenges", *Mater. Des*., **28**, 2394-2401.

Fantuzzia, N., Tornabenea, F., Bacciocchia, M. and Dimitri, R. (2017), "Free vibration analysis of arbitrarily shaped Functionally Graded Carbon Nanotube-reinforced plates", *Compos. Part B*: *Eng*., **115**, 384-408.

Fu, Y., Wang, J. and Mao, Y. (2012), "Nonlinear analysis of buckling, free vibration and dynamic stability for the piezoelectric functionally graded beams in thermal environment", *Appl. Math. Model*., **36,** 4324-4340.

Ghorbani Shenas, A., Malekzadeh, P. and Ziaee, S. (2017), "Vibration analysis of pre-twisted functionally graded carbon nanotube reinforced composite beams in thermal environment", *Compos. Struct*., **162**(15), 325-340.

Ghorbanpour Arani, A., Kolahchi, R., Mosallaie Barzoki, A.A., Mozdianfard, M.R. and Noudeh Farahani, M. (2012a), "Elastic foundation effect on nonlinear thermo-vibration of embedded double-layered orthotropic graphene sheets using differential quadrature method", *Proceedings of the Institution of Mechanical Engineers, Part C*: *J. Mech. Eng. Sci*., 1-18.

Ghorbanpour Arani, A., Vossough, H., Kolahchi, R. and Mosallaie Barzoki, A.A. (2012b), "Electro-thermo nonlocal nonlinear vibration in an embedded polymeric piezoelectric micro plate reinforced by DWBNNTs using DQM", *J. Mech. Sci. Technol*., **26** (10), 3047-3057.

Ghorbanpour Arani, A., Roudbari, M.A. and Amir, S. (2012c), "Nonlocal vibration of SWBNNT embedded in bundle of CNTs under a moving nanoparticle", *Physica B*, **407**, 3646-3653.

Ghorbanpour Arani, A., Vossough, H. and Kolahchi, R. (2015a), "Nonlinear vibration and instability of a visco-Pasternak coupled double-DWBNNTs-reinforced microplate system conveying microflow", *J. Mech. Eng. Sci*., 1-17.

Ghorbanpour Arani, A., Kolahchi, R. and Zarei, M.S. (2015b), "Visco-surface-nonlocal piezoelasticity effects on nonlinear dynamic stability of graphene sheets integrated with ZnO sensors and actuators using refined zigzag theory", *Compos. Struct*., **132**(15), 506-526.

Hichem, B., Benrahou, K.H., Bousahla, A.A. and Tounsi, A. (2017), "A nonlocal zeroth-order shear deformation theory for nonlinear postbuckling of nanobeams", *Struct. Eng. Mech., Int.*

J., **62**(6), 695-702.
Kanani, A.S., Niknam, H., Ohadi, A.R. and Aghdam, M.M. (2014), "Effect of nonlinear elastic foundation on large amplitude free and forced vibration of functionally graded beam", *Compos. Struct*., **115**, 60-68.
Ke, L.-L., Yang, J. and Kitipornchai, S. (2010), "Nonlinear free vibration of functionally graded carbon nanotube-reinforced composite beams", *Compos. Struct*., **92**, 676-683.
Khetir, H., Bouiadjra, M.B., Houari, M.S.A. and Tounsi, A. (2017), "A new nonlocal trigonometric shear deformation theory for thermal buckling analysis of embedded nanosize FG plates", *Struct. Eng. Mech., Int. J*., **64**(4), 391-402.
Kolahchi, R. and Moniri Bidgoli, A.M. (2016), "Size-dependent sinusoidal beam model for dynamic instability of single-walled carbon nanotubes", *Appl. Math. Mech. -Engl. Ed*., **37**(2), 265-274.
Kolahchi, R., Safari, M. and Esmailpour, M. (2016), "Dynamic stability analysis of temperature-dependent functionally graded CNT-reinforced visco-plates resting on orthotropic elastomeric medium", *Compos. Struct*., **150**, 255-265.
Komijani, M., Esfahani, S.E., Reddy, J.N., Liu, Y.P. and Eslami, M.R. (2014), "Nonlinear thermal stability and vibration of pre/post-buckled temperature-and microstructure-dependent functionally graded beams resting on elastic foundation", *Compos. Struct*., **112**, 292-307.
Li, L. and Hu, Y. (2016), "Wave propagation in fluid-conveying viscoelastic carbon nanotubes based on nonlocal strain gradient theory", *Comput. Mater. Sci*., **112**, 282-288.
Li, J., Wu, Z., Kong, X., Li, X. and Wu, W. (2014), "Comparison of various shear deformation theories for free vibration of laminated composite beams with general lay-ups", *Compos. Struct*., **108**, 767-778.
Li, L., Hu, Y. and Ling, L. (2015), "Wave propagation in viscoelastic single-walled carbon nanotubes with surface effect under magnetic field based on nonlocal strain gradient theory", *Physica E*, **75**, 118-124.
Liew, K.M., Yang, J. and Kitipornchai, S. (2003), "Postbuckling of piezoelectric FGM plates subject to thermo-electro-mechanical loading", *Int. J. Solids Struct*., **40**, 3869-3892.
Liew, K.M., Hu, Y.G. and He, X.Q. (2008), "Flexural wave propagation in single-walled carbon nanotubes", *J. Comput. Theor. Nanosci*., **5**(4), 581-586.
Maraghi, Z.K., Ghorbanpour Arani, A., Kolahchi, R., Amir, S. and Bagheri, M.R. (2013), "Nonlocal vibration and instability of embedded DWBNNT conveying viscose fluid", *Compos.*: *Part B*, **45**, 423-432.
Mohammadimehr, M., Rousta Navi, B. and Ghorbanpour Arani, A. (2015), "Free vibration of viscoelastic double-bonded polymeric nanocomposite plates reinforced by FG-SWCNTs using MSGT, sinusoidal shear deformation theory and meshless method", *Compos. Struct*., **131**, 654-671.
Natarajan, S., Haboussi, M. and Manickam, G. (2014), "Application of higher-order structural theory to bending and free vibration analysis of sandwich plates with CNT reinforced composite", *Compos. Struct*., **113**, 197-207.
Rafiee, M., Yang, J. and Kitipornchai, S. (2013), "Large amplitude vibration of carbon nanotube reinforced functionally graded composite beams with piezoelectric layers", *Compos. Struct*., **96**, 716-725.
Rafiee, M., He, X.Q. and Liew, K.M. (2014), "Non-linear dynamic stability of piezoelectric functionally graded carbon nanotube-reinforced composite plates with initial geometric imperfection", *Int. J. Non-Linear Mech*., **59**, 37-51.
Reddy, J.N. (2007), "Nonlocal theories for bending, buckling and vibration of beams", *Int. J. Eng. Sci*., **45**, 288-307.
Reddy, J.N. and El-Borgi, S. (2014), "Eringen's nonlocal theories of beams accounting for moderate rotations", *Int. J. Eng. Sci*., **82**, 159-177.
Shen, H.-S. and Zhang, C.-L. (2012), "Non-linear analysis of functionally graded fiber reinforced composite laminated plates, Part I: Theory and solutions", *Int. J. Non-Linear Mech*., **47**, 1045-1054.
Simsek, M. and Reddy, J.N. (2013a), "A unified higher order beam theory for buckling of a functionally graded microbeam embedded in elastic medium using modified couple stress theory", *Compos. Struct*., **101**, 47-58.
Simsek, M. and Reddy, J.N. (2013b), "Bending and vibration of functionally graded microbeams using a new higher order beam theory and the modified couple stress theory", *Int. J. Eng. Sci*., **64**, 37-53.
Tornabene, F., Fantuzzi, N., Ubertini, F. and Viola, E. (2014a), "Strong formulation finite element method based on differential quadrature: a survey", *Appl. Mech. Rev*., **67**, 020801.
Tornabene, F., Fantuzzi, N. and Bacciocchi, M. (2014b), "The strong formulation finite element method: stability and accuracy", *Frattura ed Integrità Strutturale*, **29**, 251-265.
Tornabene, F., Fantuzzi, N., Bacciocchi, M. and Viola, E. (2016), "Effect of agglomeration on the natural frequencies of functionally graded carbon nanotube-reinforced laminated composite doubly-curved shells", *Compos. Part B*: *Eng*., **89**, 187-218.
Tornabene, F., Fantuzzi, N. and Bacciocchi, M. (2017), "Linear static response of nanocomposite plates and shells reinforced by agglomerated carbon nanotubes", *Compos. Part B*: *Eng.*, **115**, 449-476.
Wu, H., Kitipornchai, S. and Yang, J. (2017), "Imperfection sensitivity of thermal post-buckling behaviour of functionally graded carbon nanotube-reinforced composite beams", *Appl. Math. Model*., **42**, 735-752.
Xua, R. and Wu, Y. (2007), "Static, dynamic, and buckling analysis of partial interaction composite members using Timoshenko's beam theory", *Int. J. Mech. Sci*., **49**, 1139-1155.
Yahia, S.A., Hassen, A.A., Mohammed Sid Ahmed, H. and Tounsi, A. (2015), "Wave propagation in functionally graded plates with porosities using various higher-order shear deformation plate theories", *Struct. Eng. Mech., Int. J*., **53**(6), 1143-1165.
Yang, Y. and Lim, C.W. (2012), "Non-classical stiffness strengthening size effects for free vibration of a nonlocal nanostructure", *Int. J. Mech. Sci*., **54**, 57-68.
Zhang, Z.J. and Paulino, G.H. (2007), "Wave propagation and dynamic analysis of smoothly graded heterogeneous continua using graded finite elements", *Int. J. Solids Struct*., **44**(11), 3601-3626.
Zidi, M., Tounsi, A., Sid Ahmed Houari, M., Adda Bedia, E.-A. and Anwar Bég, O. (2014), "Bending analysis of FGM plates under hygro-thermo-mechanical loading using a four variable refined plate theory", *Aerosp. Sci. Tech.*, **34**, 24-34.

CC

Abbreviation

FG	Functionally Graded
CNTs	Carbon Nanotubes
TSDBT	Trigonometric Shear Deformation Beam Theory
ESDBT	Exponential Shear Deformation Beam Theory
HSDBT	Hyperbolic Shear Deformation Beam Theory
ASDBT	Aydogdu Shear Deformation Beam Theory
SWCNT	Single-Walled Carbon Nanotube
CFs	Carbon Fibers
CNTRCs	Carbon Nanotube-Reinforced Composites
MEMS	Micro-Electro-Mechanical Systems
NEMS	Nano-Electro-Mechanical Systems